nature microbiology

ARTICLES

https://doi.org/10.1038/s41564-022-01158-0

Bacteria deplete deoxynucleotides to defend against bacteriophage infection

Nitzan Tal[1], Adi Millman[1], Avigail Stokar-Avihail[1], Taya Fedorenko[1], Azita Leavitt[1], Sarah Melamed[1], Erez Yirmiya[1], Carmel Avraham[1], Alexander Brandis[2], Tevie Mehlman[2], Gil Amitai[1] and Rotem Sorek[1]✉

DNA viruses and retroviruses consume large quantities of deoxynucleotides (dNTPs) when replicating. The human antiviral factor SAMHD1 takes advantage of this vulnerability in the viral lifecycle, and inhibits viral replication by degrading dNTPs into their constituent deoxynucleosides and inorganic phosphate. Here, we report that bacteria use a similar strategy to defend against bacteriophage infection. We identify a family of defensive bacterial deoxycytidine triphosphate (dCTP) deaminase proteins that convert dCTP into deoxyuracil nucleotides in response to phage infection. We also identify a family of phage resistance genes that encode deoxyguanosine triphosphatase (dGTPase) enzymes, which degrade dGTP into phosphate-free deoxyguanosine and are distant homologues of human SAMHD1. Our results suggest that bacterial defensive proteins deplete specific deoxynucleotides (either dCTP or dGTP) from the nucleotide pool during phage infection, thus starving the phage of an essential DNA building block and halting its replication. Our study shows that manipulation of the dNTP pool is a potent antiviral strategy shared by both prokaryotes and eukaryotes.

Bacteria use multiple immune mechanisms to defend against phage infection[1,2]. Restriction–modification (RM) and CRISPR–Cas systems have long been recognized as major lines of defence against phages[1]. Abortive infection systems, where infected cells commit suicide and thus abort phage propagation, have also been reported in bacteria since the early days of phage research[3].

In recent years, it has become clear that bacteria encode a plethora of additional immune systems that escaped early detection[1,2]. These include defence systems that produce small molecules which block phage replication[4,5], systems that rely on secondary-messenger signalling molecules that activate immune effectors[6–9], and retron systems that employ reverse-transcribed non-coding RNAs as part of their anti-phage activity[10,11]. Many of these recently identified bacterial immune systems were shown to be functionally and structurally homologous to immune genes that protect eukaryotic cells from infection[5,7,9,12]. Despite this recent progress in identifying bacterial defence systems, it has been hypothesized that many such systems still await discovery[13].

Cytidine deaminases confer phage defence in *Escherichia coli*

We initiated this study by focusing on a family of homologous genes, found in a broad set of bacterial genomes, which contain a predicted cytidine-deaminase domain (Fig. 1a and Extended Data Fig. 1a). This family of genes caught our attention due to their frequent localization next to known anti-phage defence systems in diverse bacterial genomes, a strong predictor for a role in anti-phage defence[14] (Extended Data Fig. 1b and Supplementary Table 1). We cloned two genes from this family, one from *Escherichia coli* U09 and the other from *E. coli* AW1.7, under the control of their native promoters, into a lab strain of *E. coli* (MG1655) that does not naturally encode such genes. Infection assays with a panel of phages showed that both genes conferred substantial defence against a diverse set of phages (Fig. 1b and Extended Data Fig. 1c). Since it conferred wider defence against phages, we further functionally characterized the gene from *E. coli* AW1.7 (Fig. 1b,c). Point mutations in the active site of the deaminase domain (C370A and C401A, predicted to disrupt zinc binding) abolished defence (Fig. 1c). In addition, point mutations in the nucleotide-binding motif of a predicted kinase domain found at the N terminus of the protein also resulted in impaired defence (Fig. 1c), suggesting that both domains are essential for the defence against phages. Expression of the gene without phage infection did not impair bacterial growth (Extended Data Fig. 1d).

Cytosine deaminase enzymatic activities have been reported for immune proteins that protect human cells from viral infection by inducing deoxycytidine-to-deoxyuridine substitutions in the DNA of the viral genome, causing hyper-mutations that destroy the coding capacity of the virus[15]. To examine whether the bacterial cytosine deaminase has a similar function, we extracted and sequenced total DNA and RNA from deaminase-containing and control strains of *E. coli* MG1655 infected with phage T7. We did not observe elevated rates of C-to-T mismatches (or the expected corresponding G-to-A in the complementary strand) as compared with other mismatches in phage DNA or RNA in cells encoding the cytidine deaminase, or as compared with control cells lacking the gene (Extended Data Fig. 2). In addition, no hyper-editing of cytosines in the DNA or RNA molecules of the bacterial host was observed (Extended Data Fig. 2). We concluded that the bacterial cytosine deaminase genes that protect against phages do so via a mechanism that does not involve hyper-editing of the nucleic-acid polymers.

Deamination of dCTP depletes it from the dNTP pool

We next examined whether the bacterial defensive protein modifies single nucleotides rather than DNA or RNA polymers. To this end, we filtered extracts from cells infected by phage T7 and used liquid chromatography followed by mass spectrometry (LC-MS) to monitor the nucleotide content in these extracts (Fig. 1d). Remarkably,

[1]Department of Molecular Genetics, Weizmann Institute of Science, Rehovot, Israel. [2]Life Sciences Core Facilities, Weizmann Institute of Science, Rehovot, Israel. ✉e-mail: rotem.sorek@weizmann.ac.il

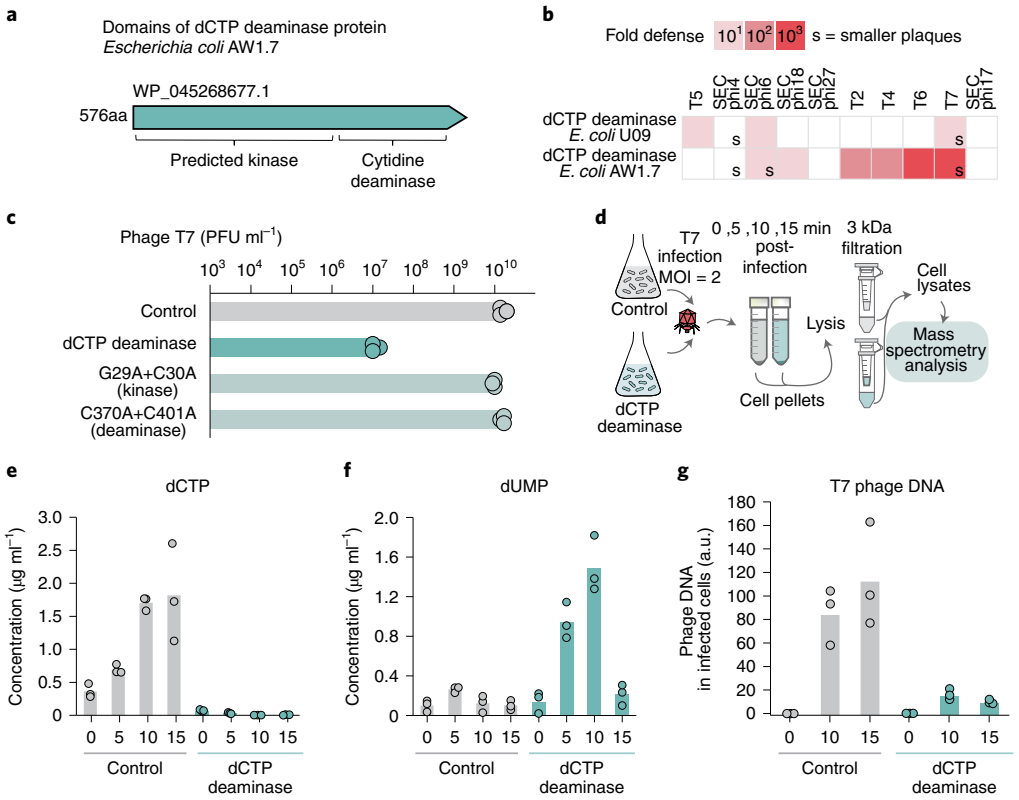

Fig. 1 | A family of cytidine deaminases provide defence against phages. a, Domain organization of the cytidine deaminase of *E. coli* AW1.7. Protein accession in the National Centre for Biotechnology Information (NCBI) is indicated above the gene. **b**, Cytidine deaminases defend against phages. Cytidine deaminases from two *E. coli* strains were cloned, together with their native promoter regions, and transformed into *E. coli* MG1655. Fold defence was measured using serial dilution plaque assays. Data represent an average of three replicates (see detailed data in Extended Data Fig. 1). The designation 's' stands for a marked reduction in plaque size. **c**, Effect of point mutations on the defensive activity of dCTP deaminase from *E. coli* AW1.7. Data represent plaque-forming units per ml (PFU ml^{-1}) of T7 phages infecting control cells, dCTP-deaminase-expressing cells, and two strains mutated in the predicted kinase or deaminase domains. Shown is the average of three replicates, with individual data points overlaid. **d**, Schematic representation of the MS experiment. **e**,**f**, Concentrations of deoxynucleotides in cell lysates extracted from T7-infected cells, as measured by LC-MS with synthesized standards. The *x* axis represents minutes post-infection, with zero representing non-infected cells. Cells were infected by phage T7 at a multiplicity of infection (MOI) of 2 at 37 °C. Each panel shows data acquired for cells expressing the dCTP deaminase from *E. coli* AW1.7 or for control cells that contain an empty vector. Bar graphs represent the average of three biological replicates, with individual data points overlaid. **g**, Effect of dCTP-deaminase on T7 DNA replication throughout infection. Cells were infected by phage T7 at an MOI of 2 at 37 °C. A fixed amount of *Bacillus subtilis* BEST7003 cells was spiked into each sample before centrifugation for normalization purposes. Total DNA was extracted from each sample and DNA was Illumina-sequenced. Each panel shows data acquired for dCTP-deaminase-expressing cells or for control cells that contain an empty vector. The *y* axis represents phage DNA sequence reads normalized to spike reads. Bar graphs represent the average of three biological replicates, with individual data points overlaid.

deoxycytidine triphosphate (dCTP), which naturally accumulates in control cells infected by phage T7, was completely absent in infected cells expressing the deaminase gene from *E. coli* AW1.7 (Fig. 1e). The depletion of dCTP was associated with substantial elevation of deoxyuridine monophosphate (dUMP), recorded as early as 5 min after initial infection, suggesting that the observed loss of dCTP was caused by its deamination into deoxyuridine compounds (Fig. 1f). Similar depletion was observed in deoxycytidine monophosphate (dCMP) and deoxycytidine diphosphate (dCDP) but not in the ribonucleotides CTP, CDP and CMP, suggesting that deamination is limited to deoxycytidines (Extended Data Fig. 3a–e). Although the deamination of dCTP is expected to generate dUTP molecules, it is known that *E. coli* expresses housekeeping deoxyuridine triphosphatase (dUTPase) enzymes that rapidly convert dUTP to dUMP molecules[16], likely explaining the observed accumulation of dUMP and not of dUTP (Fig. 1f). Indeed, a recent paper by Severin et al.[17] demonstrated the in vitro conversion of dCTP to dUTP by a dCTP deaminase enzyme of the same family. Depletion of dCTP was not observed in cells expressing dCTP deaminase mutants (Extended Data Fig. 4).

These results suggest that during infection by phage T7, the defensive deaminase protein converts deoxycytidine nucleotides into deoxyuracils, depleting the cell of the dCTP building blocks that are essential for phage DNA replication. Indeed, monitoring phage DNA during infection showed impaired phage DNA replication in deaminase-containing cells (Fig. 1g). Moreover, we observed that the other three deoxynucleotides (dNTPs), dATP, dGTP and dTTP, all accumulated in the cell at 10 and 15 min post-infection in cells expressing the dCTP deaminase (Extended Data Fig. 3f–h). These results suggest that the depletion of dCTP limits phage DNA replication, resulting in a buildup of the other dNTP building blocks that would have otherwise been incorporated into the replicating the polynucleotide chain of the phage[17].

Deoxyguanosine triphosphatases deplete dGTP during phage infection

Our discovery of a defence mechanism that uses nucleotide depletion via dCTP deamination prompted us to investigate whether there are additional phage resistance mechanisms that defend the cell by

depleting dNTPs. Depletion of the nucleotide pool was reported as an antiviral strategy in the human innate immune system, where it is manifested by the SAMHD1 antiviral protein that restricts human immunodeficiency virus (HIV) infection in non-replicating cells[18]. SAMHD1 was found to remove the triphosphate from dNTPs, breaking the nucleotides into phosphate-free deoxynucleosides and an inorganic triphosphate (PPPi)[18]. The massive degradation of dNTPs by SAMHD1 depletes the nucleotide pool of the cells and inhibits replication of the viral genome[19].

Several dNTP triphosphohydrolases (dNTPases), and specifically deoxyguanosine triphosphatases (dGTPases), have previously been described in bacteria[20–22]. Bacterial dGTPases cleave dGTP in vitro, and their structures show substantial homology to the active site architecture of SAMHD1[23,24]. Although dGTPase homologues are abundant in bacteria, their physiological roles mainly remain unknown[23]. We hypothesized that bacterial dGTPases might have a role in defence against phages through dGTP depletion.

We identified multiple genes with predicted dGTPase domains that were localized within operons of type I restriction–modification systems or near other known defence systems, suggesting a possible role in anti-phage defence[14] (Fig. 2a and Extended Data Fig. 5a). These genes could not be aligned to human SAMHD1, but structural homology modelling using AlphaFold2[25] revealed significant similarity to the structure of SAMHD1 (Extended Data Fig. 5b). To evaluate whether these genes confer phage resistance, we cloned eight of these dGTPases into *E. coli* MG1655. Following infection with a diverse set of phages, we found that six of the cloned genes substantially protected the *E. coli* host from phage infection, with the most prominent defence observed for the dGTPase from *Shewanella putrefaciens* CN-32 (*Sp*-dGTPase) (Fig. 2a,b, Extended Data Figs. 6 and 7 and Supplementary Table 5). A D101A point mutation in the histidine/aspartate (HD) motif in the predicted active site of *Sp*-dGTPase abolished defence, suggesting that the dGTPase functionality is essential for anti-phage activity (Fig. 2c). Overexpression of dGTPases did not impair bacterial growth (Extended Data Fig. 6b), and two dGTPases protected against phages when cloned under the control of their native promoters, suggesting that defence is not an artefact of overexpression (Fig. 2b and Extended Data Fig. 7a–c).

We next used LC-MS to analyse the nucleotide content in cells expressing *Sp*-dGTPase. In control cells that do not express the defensive gene, the concentration of dGTP was substantially elevated after 10 min from the onset of infection by phage T7, as expected for this phage[26] (Fig. 2d). However, in cells expressing the defensive gene, dGTP was present in lower amounts throughout the infection time course (Fig. 2d). In parallel to the depletion of dGTP, we observed substantial elevation in the concentrations of deoxyguanosine, consistent with the hypothesis that the defensive protein removes the triphosphate from dGTP (Fig. 2e). Similar reduction in dGTP levels was observed for a dGTPase from *E. coli* STEC 2595, which was cloned under the control of its native promoter (Extended Data Fig. 7). In parallel to the reduction of dGTP, the other three dNTPs accumulated in dGTP-expressing cells, and phage DNA replication was impaired (Fig. 2f and Extended Data Figs. 6e–g and 7h–k). These results reveal a family of bacterial antiviral enzymes that deplete dGTP in phage-infected cells and limit phage replication.

Numerous species encode antiviral nucleotide-depletion genes

We found 977 homologues of the defensive dCTP deaminase in 952 genomes, representing 2.5% of the set of 38,167 genomes that we analysed (Supplementary Table 1). These genes were found in genomes of a diverse set of species from the Proteobacteria phylum, as well as other phyla including Firmicutes, Actinobacteria and Bacteroidetes (Fig. 3a and Supplementary Table 1). In most cases, only a small fraction of the sequenced genomes of a given species harboured the dCTP deaminase. For example, the gene was found in 5%, 10% and 12% of analysed *E. coli*, *Legionella pneumophila*, and *Burkholderia pseudomallei* genomes, respectively (Fig. 3b). Such a sparse pattern of gene presence/absence is typical of bacterial defence systems and is indicative of extensive horizontal gene transfer between genomes[2]. An exception to this pattern was observed in *Vibrio cholerae*, where we found the defensive dCTP deaminase in most of the analysed genomes (200 of 291, 69%) (Fig. 3b).

homologues of the defensive *Sp*-dGTPase were abundant in the set of bacterial genomes that we analysed, appearing in >2,300 of the genomes (at least 25% sequence identity to *Sp*-dGTPase over an alignment overlap of ≥90%) (Supplementary Table 2). Among these, proteins that we originally tested which showed high similarity to *Sp*-dGTPase were preferentially localized next to known defence systems, implying that the main role of these direct homologues is to defend against phages (Fig. 4 and Supplementary Table 2). However, more distant homologues did not show high propensity to co-localize with defence systems, with only 10% of these homologues found next to known defensive genes (Fig. 4b and Supplementary Table 2). Experimentally examining 20 such distant homologues from across the phylogenetic tree showed that many of them (9 of 20) provided defence against phages when cloned into *E. coli* MG1655 (Fig. 4b and Extended Data Fig. 8). These findings suggest that these more distant homologues function in phage defence, but may also have housekeeping roles in bacterial physiology and are thus not encoded in defence islands. In contrast to the sparse distribution observed for dCTP deaminases, dGTPases were present in most strains of encoding species, further supporting a housekeeping role for these genes (Fig. 3c,d). In this context, it is noteworthy that SAMHD1 was found to be involved in housekeeping DNA repair, a role that has also been suggested for bacterial dGTPases[23,27].

Phages can evolve resistance to nucleotide depletion

To gain more insight into how phage infection triggers nucleotide depletion, we attempted to isolate phage mutants that escape this mode of defence. We were able to obtain four mutants of phage T7 that could partially overcome the defence conferred by the dCTP deaminase gene, as well as seven T7 mutants that overcame dGTPase defence (Supplementary Table 4). In all four mutants that escaped the dCTP deaminase, we found point mutations in gene 5.7 of phage T7, leading to amino-acid substitutions (Fig. 5a). Surprisingly, three of the T7 mutants that escaped *Sp*-dGTPase defence were also mutated in this gene, with mutations either causing frameshift in Gp5.7 or amino-acid substitutions (Fig. 5a,b). We verified that Gp5.7 is not produced during infection by a mutant phage with a frameshift in gene 5.7 using protein MS (Extended Data Fig. 9a,b). In an additional three mutants that overcame *Sp*-dGTPase, a frameshift-causing mutation was identified in gene 5.5, which is directly upstream to gene 5.7 and is thought to be co-translated with gene 5.7, forming a 5.5–5.7 fusion protein[28]. A single T7 escapee was not mutated in either of these genes, but had a point mutation in the endonuclease I gene, encoding a protein responsible for Holliday junction resolution[29] (Supplementary Table 4). These results suggest that mutations in Gp5.7 allow phage T7 to escape both the dCTP deaminase and the dGTPase defence. Indeed, escape mutants isolated on the dCTP deaminase strain were able to overcome *Sp*-dGTPase defence, and vice versa (Fig. 5c,d).

We infected dCTP-deaminase-expressing cells with the Gp5.7-mutated T7 phages, and measured dCTP concentrations. A reduction in dCTP was observed post-infection, but this reduction caused only partial, yet not full, depletion of dCTP in the infected cells (Fig. 5e). These results suggest that the nucleotide-depleting enzyme is only partially active against the mutated phages and that

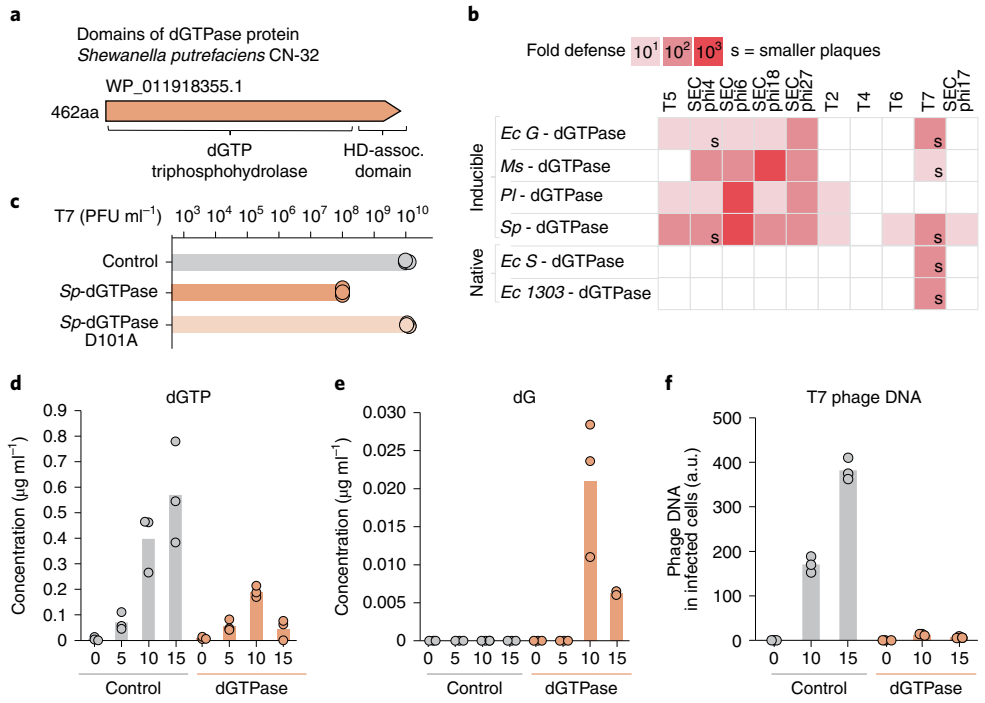

Fig. 2 | dGTPases defend against phages by depleting dGTP during phage infection. a, Domain organization of *Sp*-dGTPase. Protein accession in NCBI is indicated above the gene. **b**, Multiple dGTPases defend against phages. dGTPases were either cloned under the control of an arabinose-inducible promoter, or cloned together with their native promoter regions, and transformed into *E. coli* MG1655. Fold protection was measured using serial dilution plaque assays. Data represent the average of three replicates (see data in Extended Data Figs. 6 and 7). *Ec G*, *E. coli* G177; *Ms*, *Mesorhizobium* spp. URHA0056; *Pl*, *Pseudoalteromonas luteoviolacea* DSM6061; *Sp*, *S. putrefaciens* CN-32; *Ec S*, *E. coli* STEC 2595; *Ec 1303*, *E. coli* 1303. **c**, Plating efficiency of phage T7 on control cells, *Sp*-dGTPase-expressing cells, and a strain mutated in the predicted HD motif. Data represent PFU ml^{-1} in three replicates. **d**, Concentrations of dGTP in cell lysates extracted from T7-infected cells, as measured by LC-MS with synthesized standards. The *x* axis represents minutes post-infection, with zero representing non-infected cells. Cells were infected by phage T7 at an MOI of 2. Panel shows data acquired for *Sp*-dGTPase-expressing cells or for control cells that contain a GFP-expressing vector. Bar graphs represent the average of three biological replicates (or two replicates for dGTPase-expressing cells at 15 min), with individual data points overlaid. **e**, Concentrations of dG in cell lysates extracted from the same T7-infected cells as in panel **d**. **f**, Effect of dGTPase expression on T7 DNA replication throughout infection. Cells were infected by phage T7 at an MOI of 2 at 37 °C. Each panel shows data acquired for *Sp*-dGTPase-expressing cells or for control cells that contain a GFP-expressing vector. The *y* axis represents phage DNA sequence reads normalized to spike reads. Bar graphs represent the average of three biological replicates, with individual data points overlaid.

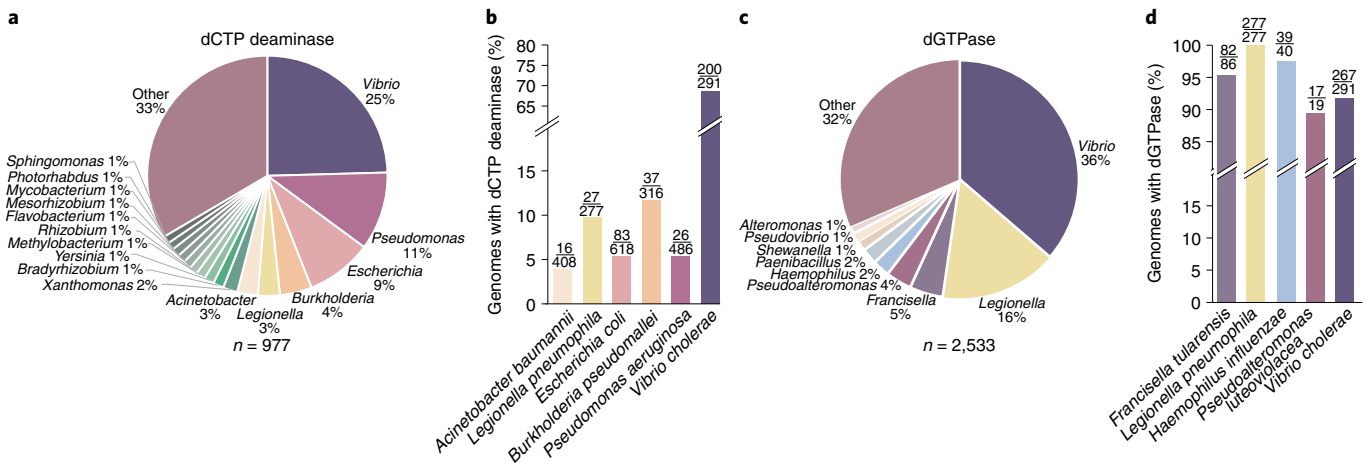

Fig. 3 | Distribution of homologues of nucleotide-depleting defence genes in bacterial genomes. a, Distribution of 977 homologues of the defensive dCTP deaminase among bacterial genomes in the analysed dataset. **b**, Presence of dCTP deaminase homologues in selected species. The values above each bar represent the number of sequenced genomes that contain the dCTP deaminase homologue out of the total number of genomes of the species present in the analysed database. **c**, Distribution of 2,533 homologues of *Sp*-dGTPases among bacterial genomes in the analysed dataset. **d**, Presence of dGTPase homologues in selected species. The values above each bar are as in **c**.

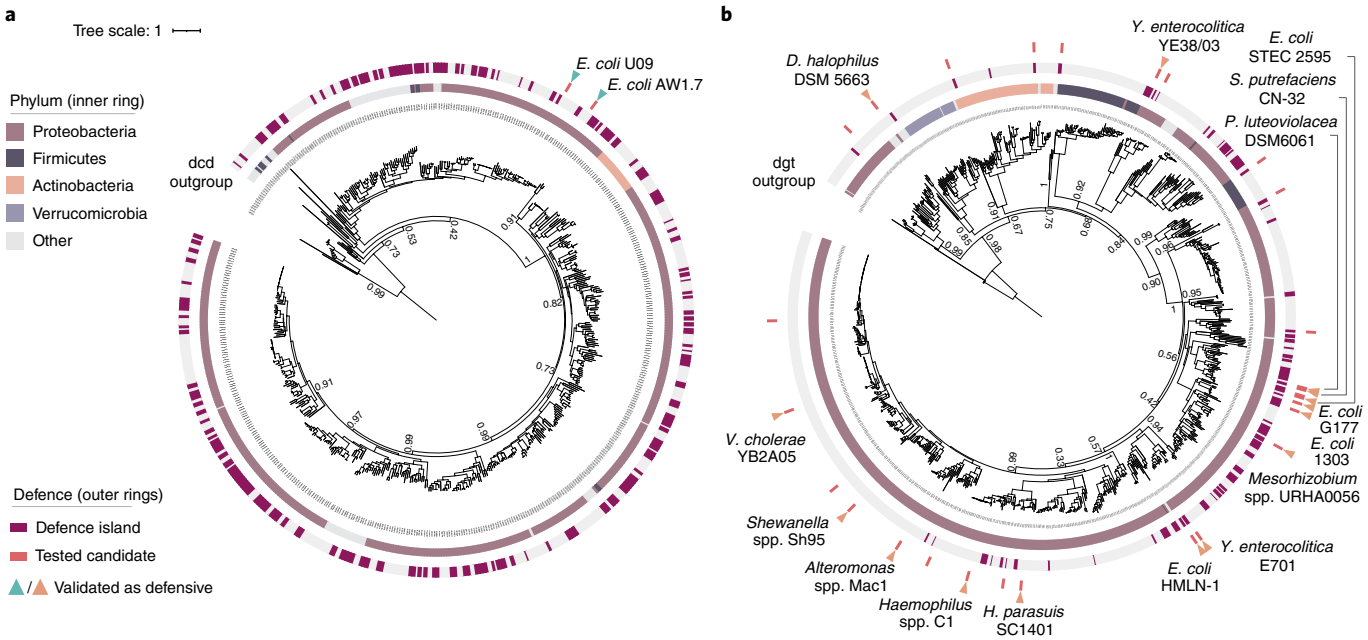

Fig. 4 | Diversity of nucleotide-depleting defence genes in bacterial genomes. a,**b**, Phylogenetic tree of dCTP deaminase (**a**) and dGTPase (**b**) homologues in prokaryotic genomes. Only non-redundant sequences were used to build the trees. The rings represent, from innermost to outermost: the phylogenetic distribution of the homologues, presence next to known defence genes, genes that were tested in this study and genes that provided defence against phages.

the remaining dCTP in the cell still allows phage DNA replication, enabling their escape from the nucleotide-depletion defence.

Gp5.7 of phage T7 is responsible for shutting down σ^S-dependent host RNA polymerase (RNAP) transcription, which would have otherwise interfered with phage propagation[30]. A second T7 protein, Gp0.7, is also known to modify the host RNAP during the early stages of infection[31]. Phages deleted in genes 0.7 or 5.7 were previously reported as viable but propagate sub-optimally on *E. coli* cells[32,33]. Intriguingly, two of the T7 mutants that escaped the *Sp*-dGTPase defence contained, in addition to the mutation in gene 5.7, mutations in gene 0.7 (Supplementary Table 4).

Our observation that mutations in phage-RNAP-modifying proteins allow T7 to escape nucleotide depletion supports a hypothesis that both the dCTP deaminase and dGTPase may be sensitive to transcription inhibition imposed during T7 phage infection. To test this hypothesis, we applied rifampicin, an antibiotic that inhibits bacterial DNA-dependent RNA polymerase, on cells expressing the dCTP deaminase or *Sp*-dGTPase. In both cases, the respective nucleotide became depleted, while the other DNA nucleotides did not (Fig. 5f,g and Extended Data Fig. 9c–h). Together, these results suggest that phage-mediated inhibition of host transcription may be involved in triggering the activation of bacterial dNTP-depletion defence (Fig. 5h).

Discussion

In this study, we describe a previously unknown mechanism of phage resistance in which phage infection triggers the activity of defensive nucleotide-manipulating enzymes that deplete one of the dNTPs from the infected cell. As phage DNA replication requires a huge supply of all of the dNTPs, reduction in or elimination of one of the dNTP pool members impairs the ability of the phage to replicate its genome. We hypothesize that nucleotide depletion might be activated when host bacteria transcription is inhibited. Many phages manipulate host transcription[34], so a mechanism of defence that relies on recognition of infection by modulation of transcription could explain the breadth of defence against multiple phage families that is conferred by the two defence genes we studied.

It is intriguing that neither of the nucleotide-depletion proteins that we studied were toxic when expressed in the host in the absence of phage infection. This suggests that while the proteins are present in the cell before phage infection, they may only be activated when a phage is recognized. Indeed, this is the case for many anti-phage defence systems, such as CBASS[7], Pycsar[35], toxin–antitoxin systems and other abortive infection systems[3] that respond to phage infection by applying lethal measures.

The dCTP deaminase analysed in our work includes a predicted N-terminal kinase domain. Point mutation in this domain abolished defence, suggesting that it is important for the defensive activity, but its specific role remains unclear. We hypothesize that this domain may participate in sensing phage infection, but its exact function remains to be defined. Housekeeping dCTP deaminase (dcd) proteins of bacteria play a role in dTTP synthesis needed for bacterial replication. The dCTP deaminase family studied here shares very little protein sequence similarity with dcd, but the two proteins share structural homology in the dCTP deaminase domain. The N-terminal kinase domain is not present in dcd proteins.

Enzymes with cytidine deaminase activity are known to be involved in multiple aspects of immunity[15]. The human APOBEC3G protects against viruses by deaminating cytosines in the viral genome, thus destroying its coding capacity[36,37]. In addition, cytosine deamination performed by activation-induced cytidine deaminase enzymes introduces somatic hyper-mutations which are essential for antibody diversification and maturation[38]. We now report a third role for cytidine deaminases in immunity, where the deamination is performed on the mononucleotide building blocks to eliminate them during viral infection. Antiviral defence by deamination of adenines was also recently demonstrated to function in defence systems that protect bacteria from phage[13].

The model *E. coli* strain MG1655 encodes a dGTPase gene called *dgt*, which shows distant homology (24% identity) to the defensive *Sp*-dGTPase studied here[39]. The function of *dgt* was linked to maintenance of genome integrity[40], although some evidence hints at a role in phage defence, as T7 was shown to encode a specific inhibitor of *dgt*[41]. It is therefore possible that families of dGTPase enzymes

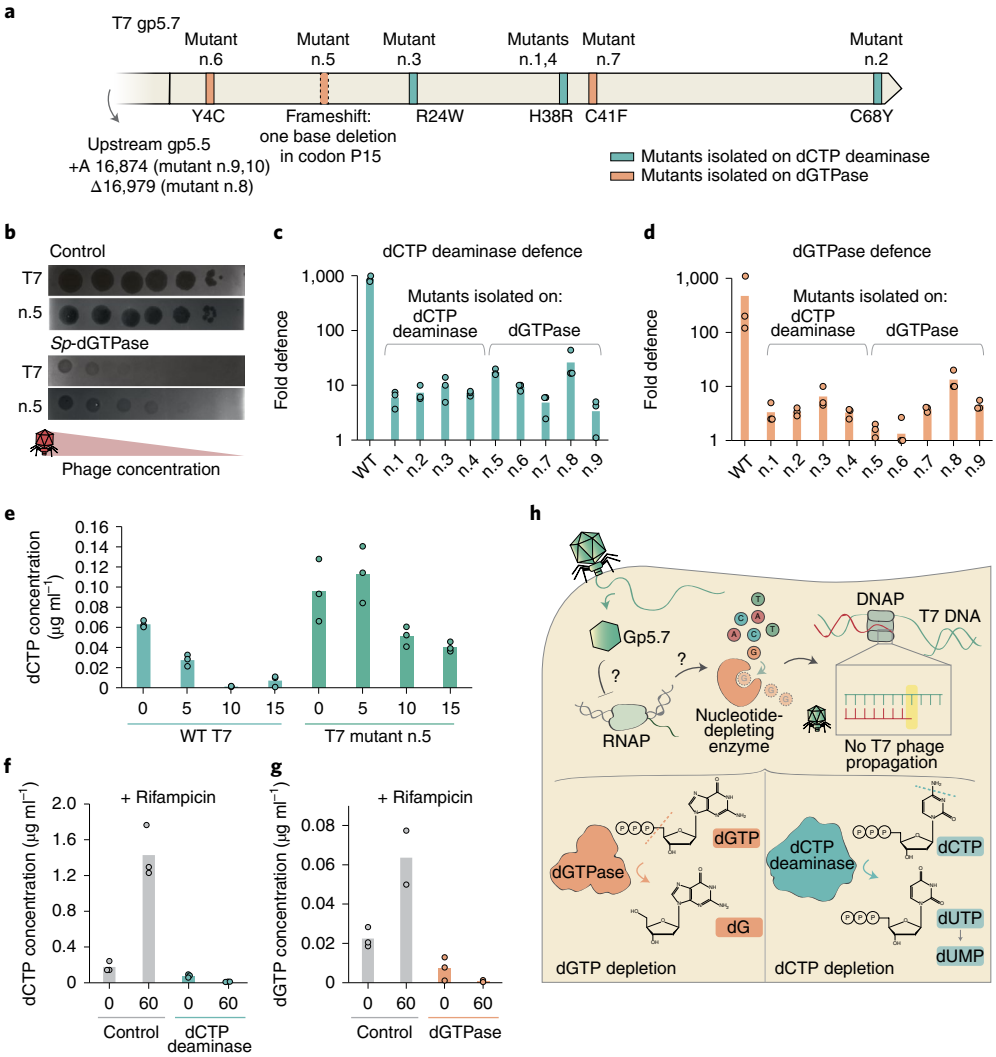

Fig. 5 | Phage mutants can overcome nucleotide-depletion defence. a, Positions in the T7 gene 5.7 that are mutated in phages that escape defence by dCTP deaminase or *Sp*-dGTPase. The full list of mutations for each phage in this figure is detailed in Supplementary Table 4. **b**, A representative phage mutant capable of escaping *Sp*-dGTPase defence. Shown are tenfold serial dilution plaque assays, comparing the plating efficiency of WT and mutant phages on bacteria that express the *Sp*-dGTPase and a control strain that lacks the system and contains a GFP-expressing vector instead. Images are representative of three replicates. **c**,**d**, Reduction of defence of dCTP deaminase (**c**) or dGTPase (**d**) when infected by the isolated phage mutants. Bacteria expressing dCTP deaminases and dGTPase, as well as a negative controls, were grown on agar plates at room temperature. Tenfold serial dilutions of the phage lysate were dropped on the plates. The *y* axis represents fold defence, calculated as the ratio between PFU ml^{-1} on control strains and on system-expressing strains. Each bar graph represents average of three replicates, with individual data points overlaid. **e**, Concentrations of dCTP in cell lysates extracted from cells expressing dCTP deaminase infected by WT T7 or T7 mutant n.5, at an MOI of 2. The *x* axis represents minutes post-infection, with zero representing non-infected cells. Bar graphs represent the average of three biological replicates, with individual data points overlaid. Data for WT T7 is the same as in Fig. 1e and presented here for comparison with mutant. **f**, dCTP concentration during rifampicin treatment on dCTP-deaminase-expressing cells, as measured by LC-MS with synthesized standards. Early-log cells were supplemented with rifampicin (concentration 100 μg ml^{-1}) and grown for 60 min. Lysates were then extracted, and dCTP concentration was measured. Bar graphs represent the average of three biological replicates, with individual data points overlaid. **g**, dGTP concentration during rifampicin treatment on dGTPase-expressing cells. Rifampicin treatment and measurements are as described in panel **f**. Bar graphs represent the average of three biological replicates (or two replicates at 60 min), with individual data points overlaid. **h**, A model for the mechanism of action of nucleotide-depleting anti-phage systems. Phage infection may be sensed by transcription shut-off, which activates a defensive enzyme to deplete a nucleotide, hence preventing further phage DNA replication and propagation.

other than the one that we studied here are also involved in phage defence.

Multiple proteins in T7 modify the host RNA polymerase (RNAP) to allow optimal infection. These include Gp0.7, Gp2 and Gp5.7. Gp0.7 is a kinase that phosphorylates σ^{70}-bound host RNAP and alters its functionality to suit phage needs[30]. At later stages of infection, Gp2 shuts off the ability of σ^{70}-RNAP to transcribe the phage genome[30]. Finally, Gp5.7 binds and inhibits transcription by σ^{S}-RNAP, which appears in the host when the cell activates the stringent response during phage infection[30]. It is intriguing that mutations in two of these RNAP-modifying proteins allow the phage to escape both mechanisms of nucleotide depletion that are characterized here (notably, Gp2 is indispensable for T7 growth and hence cannot be mutated). This implies that both the dCTP deaminase and dGTPase might somehow monitor the integrity of the host RNAP or its activity and become activated when tampered

with. Previously identified anti-phage toxin–antitoxin systems like ToxIN[42] and the hok/sok[43] killer locus were suggested to be activated by transcriptional inhibition as well. In both cases, the regulation over the toxin was achieved through an RNA molecule that, upon inhibition of transcription, declined in concentration, allowing the activity of the toxin. Indeed, a recent paper by Severin et al.[17] shows that a vibrio-encoded dCTP deaminase is regulated by a cis-acting non-coding RNA.

Our data show that nucleotide-depleting enzymes protect against various types of phage. The well-characterized phages examined in this study, including T4, T5 and T7, are known to degrade host DNA early during infection. Such DNA degradation would ultimately result in cell death, even if phage replication was prevented by the defensive enzymes. It remains to be seen whether a nucleotide-depletion mechanism could be reversible in bacteria, allowing them to survive post-phage infection, in cases where the infecting phage does not degrade host DNA.

It is plausible that additional nucleotide-depletion mechanisms exist as part of the microbial antiviral arsenal. Enzymes that degrade all four dNTPs are known to exist in multiple bacteria, including *Thermus thermophilus*, *Enterococcus faecalis* and *Pseudomonas aeruginosa*[20,22,44]. These enzymes, which have in vitro activities similar to SAMHD1, may also play a role in anti-phage defence. Moreover, nucleotide-depleting antiviral proteins may have enzymatic reactions other than nucleotide deamination or triphosphohydrolysis. We envision that nucleotide methylases, ribosyltransferases, or other nucleotide-modifying enzymes will be discovered in the future as having antiviral activities via manipulation of the nucleotide pool.

In recent years, multiple components of the human innate immune system have been shown to have evolutionary roots in bacterial defence against phages. These include the cGAS-STING pathway[45], the viperin antiviral protein[5], the argonaute protein of the RNAi machinery[46], TIR (Toll-interleukin receptor) domains[9] and gasdermin proteins[12]. The defensive dGTPases characterized in our study show distant structural homology to the SAMHD1 active site, but this homology is too limited to explain whether SAMHD1 is evolutionarily derived from a bacterial dNTPase. Regardless of the evolutionary trajectory, we find it remarkable that depletion of the nucleotide pool is a successful antiviral defence strategy shared by eukaryotes and prokaryotes alike.

Methods

Detection of nucleotide-depleting systems in defence islands. Protein sequences of all genes in 38,167 bacterial and archaeal genomes were downloaded from the Integrated Microbial Genomes (IMG) database[47] in October 2017. These proteins were filtered for redundancy using the 'clusthash' option of MMseqs2 (release 2-1c7a89)[48], using the '-min-seq-id 0.9' parameter and then clustered using the 'cluster' option, with default parameters. Each cluster with over ten genes was annotated with the most common pfam (protein family), COG (clusters of orthologous groups of proteins) and product annotations in the cluster. Defence scores were calculated as previously described[14], recording the fraction of genes in each cluster that have known defence genes in their genomic environment spanning ten genes upstream and downstream of the inspected gene. In addition, each cluster was processed using Clustal-Omega (v.1.2.4)[49] to produce a multiple-sequence alignment. The alignment of each cluster was searched using the 'hhsearch' option of hhsuite (v.3.0.3)[50] against the PDB70 and pfamA_v32 databases, using the '-p 10 -loc -z 1 -b 1 -ssm 2 -sc 1 -seq 1 -dbstrlen 10000 -maxres 32000 -M 60 -cpu 1' parameters. Clusters that had HHsearch hits[51] both to an N-terminal kinase and a C-terminal dCTP deaminase, sized >350 aa (amino acids), and which had a defence score >0.33 were included in the family of the dCTP deaminase genes studied here. Clusters sized at least ten genes, whose representative sequence[48] aligned to the representative sequences of selected dCTP deaminase clusters with an e-value <0.01, and whose size was >350aa, were also included in the family, adding 30 genes to the list in Supplementary Table 1. To generate the list of dGTPase homologues in Supplementary Table 2, we aligned the studied *Sp*-dGTPase protein to all proteins in the database using the 'search' option of MMseqs2 (release 12-113e3) using the '-s 7 -threads 20 -max-seqs 100000' parameters, and retained all hits sized >400aa that had ≥25% sequence identity to *Sp*-dGTPase, with alignment overlap of at least 90% on both query and subject sequences.

Bacterial strains and phages. *E. coli* strain MG1655 (ATCC 47076) was grown in MMB (LB (Lysogeny broth) + 0.1 mmol l^{-1} $MnCl_2$ + 5 mmol l^{-1} $MgCl_2$, with or without 0.5% agar) at 37 °C or room temperature (RT). Whenever applicable, media were supplemented with ampicillin (100 μg ml^{-1}), to ensure the maintenance of plasmids. Infection was performed in MMB media at 37 °C or RT as detailed in each section. Phages used in this study are listed in Supplementary Table 3.

Plasmid and strain construction. dCTP deaminase and dGTPase genes used in this study were synthesized by Genscript Biotech Corp. and cloned into the p15a-origin-containing pSG1 plasmid[14] with their native promoters, or into the pBad plasmid (Thermofisher, catalogue no. 43001), respectively, as previously described[5,14]. Mutants of the dCTP deaminase gene of *E. coli* AW1.7 were also synthesized and cloned by Genscript. All synthesized sequences are presented in Supplementary Table 5. Mutant of the dGTPase gene of *Shewanella putrefaciens* CN-32 was constructed using Q5 Site directed Mutagenesis kit (NEB, catalogue no. E0554S) using primers presented in Supplementary Table 6.

Plaque assays. Phages were propagated by picking a single phage plaque into a liquid culture of *E. coli* MG1655 grown at 37 °C to OD_{600} (optical density) of 0.3 in MMB (LB + 0.1 mmol l^{-1} $MnCl_2$ + 5 mmol l^{-1} $MgCl_2$) medium until culture collapse. The culture was then centrifuged for 10 min at 15,000*g* and the supernatant was filtered through a 0.2 μm filter to get rid of remaining bacteria and bacterial debris. Lysate titre was determined using the small-drop plaque assay method as described before[52].

Plaque assays were performed as previously descried[52]. Bacteria (*E. coli* MG1655 with pSG1-dCTP deaminase or pBad-dGTPase) and negative control (*E. coli* MG1655 with empty pSG1 or pBad-GFP) were grown overnight at 37 °C. Then, 300 μl of the bacterial culture was mixed with 30 ml melted MMB agar (LB + 0.1 mmol l^{-1} $MnCl_2$ + 5 mmol l^{-1} $MgCl_2$ + 0.5% agar, with or without 0.02% arabinose) and left to dry for 1 h at RT. Tenfold serial dilutions in MMB were performed for each of the tested phages and 10 μl drops were put on the bacterial layer. Plates were incubated overnight at RT. Plaque-forming units (PFUs) were determined by counting the derived plaques after overnight incubation.

Liquid culture growth. Overnight cultures of bacteria harbouring the *Sp*-dGTPase gene or a control strain harbouring a pBAD-GFP plasmid were diluted 1:100 in MMB medium, supplemented with 0.2% arabinose. Cells were incubated at 37 °C, while shaking at 200 r.p.m. for 1 h. Then 180 μl of the bacterial culture was transferred into each well of a 96-well plate and incubated at 37 °C, with shaking in a TECAN Infinite200 plate reader. OD_{600} was followed with measurement every 10 min using the TECAN iControl v.3.8.2.0 software.

DNA and RNA editing assays. Overnight cultures of bacteria (*E. coli* MG1655 harbouring pSG1-dCTP deaminase plasmid) or negative control (*E. coli* MG1655 with the pSG1 plasmid) were diluted 1:100 in 60 ml of MMB medium and incubated at 37 °C while shaking at 200 r.p.m. until early-log phase (OD_{600} of 0.3). Then 10 ml samples of each bacterial culture were taken and centrifuged at 15,000*g* for 5 min at 4 °C. The pellets were flash frozen using dry ice and ethanol. The remaining cultures were infected by phage T7 at a final MOI of 2. Samples of 10 ml were taken throughout infection at 5, 10 and 15 min post-infection, and centrifuged and flash frozen as described above.

DNA of all samples was extracted using the QIAGEN DNeasy blood and tissue kit (catalogue no. 69504), using the Gram-negative bacteria protocol. Libraries were prepared for Illumina sequencing using a modified Nextera protocol as previously described[53]. Following sequencing on an Illumina NextSeq500, the sequence reads were aligned to bacterial and phage reference genomes (GenBank accession numbers: NC_000913.3, NC_001604.1, respectively) by using NovoAlign (Novocraft) v.3.02.02 with default parameters, and mutations were identified and quantified by counting each mismatch across the genome. Frequency of mismatches was compared between control and dCTP deaminase samples throughout the infection time course.

RNA extraction was performed as described previously[54]. Briefly, frozen pellets were re-suspended in 1 ml of RNA protect solution (FastPrep) and lysed by Fastprep homogenizer (MP Biomedicals). RNA was extracted using the FastRNA PRO blue kit (MP Biomedicals, 116025050) according to the manufacturer's instructions. DNase treatment was performed using the Turbo DNA-free Kit (Life Technologies, AM2238). RNA was subsequently fragmented using fragmentation buffer (Ambion-Invitrogen, catalogue no. 10136824) at 72 °C for 1 min and 45 s. The reactions were cleaned by adding ×2.5 SPRI (solid-phase reversible immobilization) beads (Agencourt AMPure XP, Beckman-Coulter, A63881). The beads were washed twice with 80% ethanol and air dried for 5 min. The RNA was eluted using H_2O. Ribosomal RNA was depleted by using the Ribo-Zero rRNA Removal Kit (epicentre, MRZB12424). Strand-specific RNA-seq was performed using the NEBNext Ultra Directional RNA Library Prep Kit (NEB, E7420) with the following adjustments: all cleanup stages were performed using ×1.8 SPRI beads, and only one cleanup step was performed after the end repair step. Following sequencing on an Illumina NextSeq500, sequenced reads were demultiplexed and adaptors were trimmed using 'fastx clipper' software with default parameters. Reads were mapped to the bacterial and phage genomes by using NovoAlign

v.3.02.02 with default parameters, discarding reads that were non-uniquely mapped as previously described[54]. Mutations from reference genomes were identified and quantified by counting each mismatch across the transcriptome. Frequency of mismatches was compared between control and dCTP deaminase samples throughout the infection time course.

Cell lysate preparation. Overnight cultures of *E. coli* harbouring the defensive gene and negative controls were diluted 1:100 in 250 ml MMB medium (with or without 0.02% arabinose, as described in Supplementary Table 5) and grown at 37 °C (250 r.p.m.) until reaching OD_{600} of 0.3. The cultures were infected by WT (wild type) T7 phage or mutants where indicated) at a final MOI of 2. Following the addition of phage, at 5, 10 and 15 min post-infection (plus an uninfected control sample), 50 ml samples were taken and centrifuged for 5 min at 15,000*g*. Pellets were flash frozen using dry ice and ethanol. The pellets were re-suspended in 600 µl of 100 mmol l^{-1} phosphate buffer at pH = 8 and supplemented with 4 mg ml^{-1} lysozyme. The samples were then transferred to a FastPrep Lysing Matrix B 2 ml tube (MP Biomedicals, catalogue no. 116911100) and lysed using a FastPrep bead beater for 40 s at 6 m s^{-1} (two cycles). Tubes were then centrifuged at 4 °C for 15 min at 15,000*g*. Supernatant was transferred to Amicon Ultra-0.5 Centrifugal Filter Unit 3 kDa (Merck Millipore, catalogue no. UFC500396) and centrifuged for 45 min at 4 °C at 12,000*g*. Filtrate was taken and used for LC-MS analysis.

Quantification of nucleotides by HPLC-MS. Cell lysates were prepared as described above and sent for analysis at the Targeted Metabolomics unit of the Weizmann institute. Quantification of nucleotides was carried out using an Acquity I-class UPLC system coupled to Xevo TQ-S triple quadrupole mass spectrometer (both Waters). The UPLC was performed using a SeQuant ZIC-pHILIC column as described previously[55], with linear gradient decrease of acetonitrile in 20 mmol l^{-1} ammonium carbonate for 10 min. Mass spectrometry analysis was performed using electrospray interface in positive ionization mode for all metabolites, except for uracil-containing metabolites. Metabolites were detected using multiple-reaction monitoring (MRM), using argon as the collision gas. Quantification was made using a standard curve in the 0–10 µg ml^{-1} concentration range. $^{15}N_5$-AMP and $^{13}C_{10}$-ATP (both Sigma) were added to standards and samples as internal standards (0.5 µmol l^{-1} and 100 µmol l^{-1}, respectively). TargetLynx (Waters) was used for data analysis.

Isolation of mutant phages. To isolate mutant phages that escape dCTP deaminase and dGTPase defence, phages were plated on bacteria expressing each defence system using the double-layer plaque assay[56]. Bacterial cells expressing each defence system were grown in MMB (supplemented with 0.2% arabinose for the dGTPase) to an OD_{600} of 0.3. Then, 100 µl of phage lysate was mixed with 100 µl bacterial cells expressing each defence gene, and left at RT for 10 min. Then, 5 ml of pre-melted 0.5% MMB (supplemented with 0.2% arabinose for the dGTPase) was added and the mixture was poured onto a bottom layer of 1.1% MMB. For the dGTPase, the double-layer plates were incubated overnight at 37 °C, and single plaques were picked into 90 ml phage buffer. For the dCTP deaminase, double-layer plates were incubated overnight at RT and the entire top layer was scraped into 2 ml of phage buffer to enrich for phages that escape the defence genes. Phages were left for 1 h at RT during which the phages were mixed several times by vortex to release them from the agar into the phage buffer. The phages were centrifuged at 3,200*g* for 10 min to get rid of agar and bacterial cells, and the supernatant was transferred to a new tube. For both defence genes, to test the phages for the ability to escape from the defence system, the small-drop plaque assay was used[52]. A total of 300 ml bacteria harbouring the defensive gene or negative control (*E. coli* MG1655 with plasmid pSG1 or pBad-GFP lacking the system) were mixed with 30 ml melted MMB 0.5% agar and left to dry for 1 h at RT. Tenfold serial dilutions in phage buffer were performed for the ancestor phages (WT phage used for the original double-layer plaque assay) and the phages formed on the strain expressing the defence genes; 10 µl drops were put on the bacterial layer. The plates were incubated overnight at RT or 37 °C for dCTP deaminase or dGTPase, respectively.

Amplification of mutant phages. Isolated phages for which there was decreased defence compared with the ancestor phage were further propagated by picking a single plaque formed on the defence gene in the small-drop plaque assay into a liquid culture of *E. coli* harbouring the defensive gene, which was grown at 37 °C in MMB with shaking at 200 r.p.m. to an OD_{600} of 0.3. The phages were incubated with the bacteria at 37 °C with shaking at 200 r.p.m. for 3 h and then an additional 9 ml of bacterial culture grown to OD_{600} of 0.3 in MMB was added and incubated for an additional 3 h in the same conditions. For the dGTPase system, the growth media was supplemented with 0.2% arabinose throughout the entire amplification process. The lysates were then centrifuged at 15,000*g* for 10 min, and the supernatant was filtered through a 0.2 µm filter to get rid of the remaining bacteria. Phage titre was then checked using the small-drop plaque assay on the negative-control strain as described above.

Sequencing and genome analysis of phage mutants. High-titre phage lysates (>10^7 PFU ml^{-1}) of the ancestor phage and isolated phage mutants were used for DNA extraction. An amount of 0.5 ml of phage lysate was treated with DNase-I (Merck catalogue no. 11284932001) added to a final concentration of 20 µg ml^{-1} and incubated at 37 °C for 1 h to remove bacterial DNA. DNA was extracted using the QIAGEN DNeasy blood and tissue kit (catalogue no. 69504) starting from a proteinase-K treatment to degrade the phage capsids. Libraries were prepared for Illumina sequencing using a modified Nextera protocol as described above. Following sequencing on Illumina NextSeq500, reads were aligned to the phage reference genome (GenBank accession number: NC_001604.1) and mutations compared with the reference genome were identified using Breseq (v.0.29.0 or v.0.34.1 for mutant phages that escape dCTP deaminase and dGTPase, respectively) with default parameters[57]. Only mutations that occurred in the isolated mutants, but not in the ancestor phage, were considered. Silent mutations within protein-coding regions were disregarded as well.

Protein mass spectrometry. For MS of mutant gp5.7 phage, overnight cultures of *E. coli* MG1655 were diluted 1:100 in 250 ml MMB medium and grown at 37 °C (250 r.p.m.) until reaching OD_{600} of 0.3. The cultures were infected by T7 (WT phage or T7 mutant n.5) at a final MOI of 2. Following the addition of phage, at 15 min post-infection, 50 ml samples were taken and centrifuged for 5 min at 15,000*g*. For protein MS of cells expressing the dGTPase proteins, overnight cultures *E. coli* MG1655 expressing the *Sp*-dGTPase (as well as control cells expressing GFP) were diluted 1:100 in 100 ml MMB medium supplemented with 0.02% arabinose, and grown at 37 °C (250 r.p.m.) until reaching OD_{600} of 0.3. Quantities of 50 ml samples were taken and centrifuged for 5 min at 15,000*g*. Pellets were flash frozen using dry ice and ethanol. The cell pellets were subjected to lysis and in solution tryptic digestion using the S-Trap method (Protifi). The resulting peptides were analysed using nanoflow liquid chromatography (nanoAcquity) coupled to high resolution, high mass accuracy mass spectrometry (Q-Exactive HF). Each sample was analysed on the instrument separately in a random order in discovery mode. Raw data were processed with MaxQuant v.1.6.6.0. The data were searched with the Andromeda search engine against a database containing protein sequences of the WT and mutant protein sequences provided, the *E. coli* K12 and T7 protein databases as downloaded from Uniprot, and a list of common lab contaminants. The following modifications were defined for the search: fixed modification was cysteine carbamidomethylation; variable modifications were methionine oxidation, asparagine and glutamine deamidation. The quantitative comparisons were calculated using Perseus v.1.6.0.7. Decoy hits were filtered out.

Rifampicin assay. Overnight cultures of *E. coli* harbouring the defensive gene and negative controls were diluted 1:100 in MMB medium (with or without 0.02% arabinose, as described in Supplementary Table 5) and grown at 37 °C (250 r.p.m.) until reaching OD_{600} of 0.3 (for dCTP deaminase-expressing cells) or OD_{600} of 0.6 (for dGTPase-expressing cells). The cultures were supplemented with rifampicin to a final concentration of 100 µg ml^{-1}. At 60 min post-addition of rifampicin (as well as an untreated control), 50 ml samples were taken and centrifuged for 5 min at 15,000*g*. Pellets were flash frozen using dry ice and ethanol. The pellets were re-suspended in 600 µl of 100 mmol l^{-1} phosphate buffer at pH = 8 and supplemented with 4 mg ml^{-1} lysozyme. The samples were then transferred to a FastPrep Lysing Matrix B 2 ml tube (MP Biomedicals catalogue no. 116911100) and lysed using a FastPrep bead beater for 40 s at 6 m s^{-1} (two cycles). Tubes were then centrifuged at 4 °C for 15 m at 15,000*g*. Supernatant was transferred to the Amicon Ultra-0.5 Centrifugal Filter Unit 3 kDa (Merck Millipore catalogue no. UFC500396) and centrifuged for 45 min at 4 °C at 12,000*g*. Filtrate was taken and used for LC-MS analysis as described above.

DNA replication assay. Overnight cultures of *E. coli* harbouring the defensive gene and negative controls were diluted 1:100 in MMB medium (with or without 0.02% arabinose, as described in Supplementary Table 5) and incubated at 37 °C while shaking at 200 r.p.m. until early-log phase (OD_{600} of 0.3). For dCTP deaminase, *Sp*-dGTPase-expressing cells and their controls' 10 ml samples of each bacterial culture were taken and spiked with 0.5 ml of *B. subtilis* BEST7003 (stationary phase, diluted 1:10), and centrifuged at 15,000*g* for 5 min at 4 °C. The pellets were flash frozen using dry ice and ethanol. The remaining cultures were infected by phage T7 at a final MOI of 2. Quantities of 10 ml samples were taken at 10 and 15 min post-infection, and spiked with 0.5 ml *B. subtilis* BEST7003 before centrifugation. Samples were flash frozen as described above. For *Ec-S*-dGTPase-expressing cells and their controls, 10 ml samples of each bacterial culture were taken and centrifuged at 15,000 x g for 5 min at 4 °C. The pellets were flash frozen using dry ice and ethanol. The remaining cultures were infected by phage T7 at a final MOI of 2. Then 10 ml samples were taken at 10 and 15 min post-infection. Samples were flash frozen as described above.

DNA of all samples was extracted using the QIAGEN DNeasy blood and tissue kit (catalogue no. 69504), using the Gram-negative bacteria protocol. Libraries were prepared for Illumina sequencing using a modified Nextera protocol as previously described[53]. For *Ec-S*-dGTPase-expressing cells and their controls, 20 ng of *Salinispora pacifica* 45547 purified DNA was spiked in, following DNA extraction for normalization purposes. Following sequencing on an Illumina NextSeq500 the sequence reads were aligned to *E. coli* MG1655, *B. subtilis* BEST7003 and phage reference genomes (GenBank accession numbers:

NC_000913.3, AP012496 and NC_001604.1, respectively) by using NovoAlign v.3.02.02 with default parameters. The number of reads mapped to *E. coli* and T7 genomes were normalized to the number of spike reads mapped to *B. subtilis* or *S. pacifica* 45547 genome, as mentioned above.

Phylogenetic analysis. To generate the phylogenetic trees in Fig. 4 the 'clusthash' option of MMseqs2 (ref. [48]; release 6-f5a1c) was used to remove protein redundancies (using the '–min-seq-id 0.9' parameter). Sequences of the defensive genes were aligned using clustal-omega v.1.2.4 with default parameters[58]. FastTree was used to generate a tree from the multiple-sequence alignment using default parameters[59]. iTOL was used for tree visualization[60]. For dCTP deaminase, 11 sequences of dcd housekeeping proteins were added (IMG ID: 2626483291, 2647195735, 2630603045, 2650338752, 2687266570, 2686871019, 2513211955, 2506703112, 2659712595, 2687072778, 2671786882) and used as an outgroup. For dGTPase, six sequences of dgt housekeeping proteins were added (IMG ID: 2875679221, 2908557952, 2908562675, 2909293708, 2913142694, 2913158190) and used as an outgroup.

Statistics and reproducibility. No statistical method was used to pre-determine sample size. Experiments were performed in triplicates unless stated otherwise. Randomization was used for sample injection order in MS measurements. No data were excluded from the analyses unless stated otherwise in figure legends.

Reporting summary. Further information on research design is available in the Nature Research Reporting Summary linked to this article.

Data availability

Data that support the findings of this study are available in the Article and its Extended Data. Gene accessions appear in the Methods section of the paper. DNA and RNA sequencing data used in Extended Data Fig. 2 can be found in the European Nucleotide Archive (ENA) ID: ERA11772567. Source data are provided with this paper. Additional data are available from the corresponding authors upon request.

Received: 16 December 2021; Accepted: 23 May 2022;
Published online: 11 July 2022

References

1. Hampton, H. G., Watson, B. N. J. & Fineran, P. C. The arms race between bacteria and their phage foes. *Nature* **577**, 327–336 (2020).
2. Bernheim, A. & Sorek, R. The pan-immune system of bacteria: antiviral defence as a community resource. *Nat. Rev. Microbiol.* **18**, 113–119 (2020).
3. Lopatina, A., Tal, N. & Sorek, R. Abortive infection: bacterial suicide as an antiviral immune strategy. *Annu. Rev. Virol.* **7**, 371–384 (2020).
4. Kronheim, S. et al. A chemical defence against phage infection. *Nature* **564**, 283–286 (2018).
5. Bernheim, A. et al. Prokaryotic viperins produce diverse antiviral molecules. *Nature* **589**, 120–124 (2021).
6. Lowey, B. et al. CBASS Immunity uses CARF-related effectors to sense 3′–5′- and 2′–5′-linked cyclic oligonucleotide signals and protect bacteria from phage infection. *Cell* **182**, 38–49.e17 (2020).
7. Cohen, D. et al. Cyclic GMP–AMP signalling protects bacteria against viral infection. *Nature* **574**, 691–695 (2019).
8. Lau, R. K. et al. Structure and mechanism of a cyclic trinucleotide-activated bacterial endonuclease mediating bacteriophage immunity. *Mol. Cell* **77**, 723–733.e6 (2020).
9. Ofir, G. et al. Antiviral activity of bacterial TIR domains via immune signalling molecules. *Nature* **600**, 116–120 (2021).
10. Millman, A. et al. Bacterial retrons function in anti-phage defense. *Cell* **183**, 1551–1561.e12 (2020).
11. Bobonis, J. et al. Bacterial retrons encode tripartite toxin/antitoxin systems. Preprint at *bioRxiv* https://doi.org/10.1101/2020.06.22.160168 (2020).
12. Johnson, A. G. et al. Bacterial gasdermins reveal an ancient mechanism of cell death. *Science* **375**, 221–225 (2022).
13. Gao, L. et al. Diverse enzymatic activities mediate antiviral immunity in prokaryotes. *Science* **369**, 1077–1084 (2020).
14. Doron, S. et al. Systematic discovery of antiphage defense systems in the microbial pangenome. *Science* **359**, eaar4120 (2018).
15. Harris, R. S. & Dudley, J. P. APOBECs and virus restriction. *Virology* **479–480**, 131–145 (2015).
16. Vértessy, B. G. & Tóth, J. Keeping uracil out of DNA: physiological role, structure and catalytic mechanism of dUTPases. *Acc. Chem. Res.* **42**, 97–106 (2009).
17. Severin, G. B. et al. A broadly conserved deoxycytidine deaminase protects bacteria from phage infection. Preprint at *bioRxiv* https://doi.org/10.1101/2021.03.31.437871 (2021).
18. Goldstone, D. C. et al. HIV-1 restriction factor SAMHD1 is a deoxynucleoside triphosphate triphosphohydrolase. *Nature* **480**, 379–382 (2011).
19. Ayinde, D., Casartelli, N. & Schwartz, O. Restricting HIV the SAMHD1 way: through nucleotide starvation. *Nat. Rev. Microbiol.* **10**, 675–680 (2012).
20. Quirk, S. & Bessman, M. J. dGTP triphosphohydrolase, a unique enzyme confined to members of the family Enterobacteriaceae. *J. Bacteriol.* **173**, 6665–6669 (1991).
21. Kondo, N. et al. Structure of dNTP-inducible dNTP triphosphohydrolase: insight into broad specificity for dNTPs and triphosphohydrolase-type hydrolysis. *Acta Crystallogr., Sect. D: Biol. Crystallogr.* **63**, 230–239 (2007).
22. Mega, R., Kondo, N., Nakagawa, N., Kuramitsu, S. & Masui, R. Two dNTP triphosphohydrolases from Pseudomonas aeruginosa possess diverse substrate specificities. *FEBS J.* **276**, 3211–3221 (2009).
23. Singh, D. et al. Structure of Escherichia coli dGTP triphosphohydrolase: a hexameric enzyme with DNA effector molecules. *J. Biol. Chem.* **290**, 10418–10429 (2015).
24. Barnes, C. O. et al. The crystal structure of dGTPase reveals the molecular basis of dGTP selectivity. *Proc. Natl Acad. Sci. USA* **116**, 9333–9339 (2019).
25. Jumper, J. et al. Highly accurate protein structure prediction with AlphaFold. *Nature* https://doi.org/10.1038/s41586-021-03819-2 (2021).
26. Lee, S. J. & Richardson, C. C. Choreography of bacteriophage T7 DNA replication. *Curr. Opin. Chem. Biol.* **15**, 580–586 (2011).
27. Daddacha, W. et al. SAMHD1 Promotes DNA end resection to facilitate DNA repair by homologous recombination. *Cell Rep.* **20**, 1921–1935 (2017).
28. Dunn, J. J., Studier, F. W. & Gottesman, M. Complete nucleotide sequence of bacteriophage T7 DNA and the locations of T7 genetic elements. *J. Mol. Biol.* **166**, 477–535 (1983).
29. Hadden, J. M., Déclais, A. C., Carr, S. B., Lilley, D. M. J. & Phillips, S. E. V. The structural basis of Holliday junction resolution by T7 endonuclease I. *Nature* **449**, 621–624 (2007).
30. Tabib-Salazar, A. et al. T7 phage factor required for managing RpoS in Escherichia coli. *Proc. Natl Acad. Sci. USA* **115**, E5353–E5362 (2018).
31. Severinova, E. & Severinov, K. Localization of the Escherichia coli RNA polymerase β′ subunit residue phosphorylated by bacteriophage T7 kinase Gp0.7. *J. Bacteriol.* **188**, 3470–3476 (2006).
32. Tabib-Salazar, A. et al. Full shut-off of Escherichia coli RNA-polymerase by T7 phage requires a small phage-encoded DNA-binding protein. *Nucleic Acids Res.* **45**, 7697–7707 (2017).
33. Hirsch-Kauffmann, M., Hherrlich, P., Ponta, H. & Schweiger, M. Helper function of T7 protein kinase in virus propagation. *Nature* **255**, 508–510 (1975).
34. Nechaev, S. & Severinov, K. Bacteriophage-induced modifications of host RNA polymerase. *Annu. Rev. Microbiol.* **57**, 301–322 (2003).
35. Tal, N. et al. Cyclic CMP and cyclic UMP mediate bacterial immunity against phages. *Cell* **184**, 5728–5739 (2021).
36. Okada, A. & Iwatani, Y. APOBEC3G-mediated G-to-A hypermutation of the HIV-1 genome: the missing link in antiviral molecular mechanisms. *Front. Microbiol.* **7**, 2027 (2016).
37. Stavrou, S. & Ross, S. R. APOBEC3 proteins in viral immunity. *J. Immunol.* **195**, 4565–4570 (2015).
38. Kumar, R., DiMenna, L. J., Chaudhuri, J. & Evans, T. Biological function of activation-induced cytidine deaminase (AID). *Biomed. J.* **37**, 269–283 (2014).
39. Wurgler, S. M. & Richardson, C. C. Structure and regulation of the gene for dGTP triphosphohydrolase from Escherichia coli. *Proc. Natl Acad. Sci. USA* **87**, 2740–2744 (1990).
40. Gawel, D., Hamilton, M. D. & Schaaper, R. M. A novel mutator of Escherichia coli carrying a defect in the dgt gene, encoding a dGTP triphosphohydrolase. *J. Bacteriol.* **190**, 6931–6939 (2008).
41. Myers, J. A., Beauchamp, B. B. & Richardson, C. C. Gene 1.2 protein of bacteriophage T7. Effect on deoxyribonucleotide pools. *J. Biol. Chem.* **262**, 5288–5292 (1987).
42. Fineran, P. C. et al. The phage abortive infection system, ToxIN, functions as a protein-RNA toxin-antitoxin pair. *Proc. Natl Acad. Sci. USA* **106**, 894–899 (2009).
43. Pecota, D. C. & Wood, T. K. Exclusion of T4 Phage by the hok/sok killer locus from plasmid R1. *J. Bacteriol.* **178**, 2044–2050 (1996).
44. Kondo, N. et al. Insights into different dependence of dNTP triphosphohydrolase on metal ion species from intracellular ion concentrations in Thermus thermophilus. *Extremophiles* **12**, 217–223 (2008).
45. Morehouse, B. R. et al. STING cyclic dinucleotide sensing originated in bacteria. *Nature* **586**, 429–433 (2020).
46. Kuzmenko, A. et al. DNA targeting and interference by a bacterial Argonaute nuclease. *Nature* **587**, 632–637 (2020).
47. Chen, I. M. A. et al. IMG/M v.5.0: an integrated data management and comparative analysis system for microbial genomes and microbiomes. *Nucleic Acids Res.* **47**, D666–D677 (2019).
48. Steinegger, M. & Söding, J. MMseqs2 enables sensitive protein sequence searching for the analysis of massive data sets. *Nat. Biotechnol.* **35**, 1026–1028 (2017).
49. Sievers, F. et al. Fast, scalable generation of high-quality protein multiple sequence alignments using Clustal Omega. *Mol. Syst. Biol.* **7**, 539 (2011).

50. Soding, J. Protein homology detection by HMM-HMM comparison. *Bioinformatics* **21**, 951–960 (2005).
51. Zimmermann, L. et al. A completely reimplemented MPI bioinformatics toolkit with a new HHpred server at its core. *J. Mol. Biol.* **430**, 2237–2243 (2018).
52. Mazzocco, A., Waddell, T. E., Lingohr, E. & Johnson, R. P. Enumeration of bacteriophages using the small drop plaque assay system. *Methods Mol. Biol.* **501**, 81–85 (2009).
53. Baym, M. et al. Inexpensive multiplexed library preparation for megabase-sized genomes. *PLoS ONE* **10**, e0128036 (2015).
54. Dar, D. et al. Term-seq reveals abundant ribo-regulation of antibiotics resistance in bacteria. *Science* **352**, aad9822–aad9822 (2016).
55. Joo Sang, L. et al. Urea cycle dysregulation generates clinically relevant genomic and biochemical signatures. *Cell* **174**, 1559–1570.e22 (2018).
56. Kropinski, A. M., Mazzocco, A., Waddell, T. E., Lingohr, E. & Johnson, R. P. Enumeration of bacteriophages by double agar overlay plaque assay. *Methods Mol. Biol.* **501**, 69–76 (2009).
57. Deatherage, D. E. & Barrick, J. E. Identification of mutations in laboratory-evolved microbes from next-generation sequencing data using breseq. *Methods Mol. Biol.* **1151**, 165–188 (2014).
58. Sievers, F. & Higgins, D. G. Clustal omega for making accurate alignments of many protein sequences. *Protein Sci.* **27**, 135–145 (2018).
59. Price, M. N., Dehal, P. S. & Arkin, A. P. Fasttree: computing large minimum evolution trees with profiles instead of a distance matrix. *Mol. Biol. Evol.* **26**, 1641–1650 (2009).
60. Letunic, I. & Bork, P. Interactive Tree of Life (iTOL) v4: recent updates and new developments. *Nucleic Acids Res.* **47**, W256–W259 (2019).

Acknowledgements

We would like to thank P. Cossart for directing us to the SAMHD1 antiviral mechanism, and A. Bernheim and the Sorek laboratory members for comments on earlier versions of this manuscript and fruitful discussion. R.S. was supported, in part, by the European Research Council (grant no. ERC-CoG 681203), Israel Science Foundation (grant no. ISF 296/21), the Deutsche Forschungsgemeinschaft (SPP 2330, grant no. 464312965), the Ernest and Bonnie Beutler Research Programme of Excellence in Genomic Medicine, the Minerva Foundation with funding from the Federal German Ministry for Education and Research, the Knell Family Centre for Microbiology, the Yotam project and the Weizmann Institute Sustainability And Energy Research (SAERI) initiative, and the Dr Barry Sherman Institute for Medicinal Chemistry. A.M. was supported by a fellowship from the Ariane de Rothschild Women Doctoral Programme and, in part, by the Israeli Council for Higher Education via the Weizmann Data Science Research Centre, and by a research grant from Madame Olga Klein-Astrachan. Protein MS was performed at the Weizmann De Botton Protein Profiling Institute.

Author contributions

N.T. and R.S. led the study and performed all analyses and experiments unless otherwise indicated. N.T. performed the genetic analyses and the in vivo experimental assays and analysed the data. A.M., E.Y. and N.T. performed the computational analyses of systems prediction. A.S-A. designed and executed the mutant-phage isolation experiments and their analysis. C.A. assisted with plaque assays and DNA isolation of mutant phages. T.F. assisted with isolation of mutant phages and in conducting plaque assays. A.L. and S.M. assisted in conducting plaque assays and preparing DNA sequencing libraries. G.A. assisted with sequence analysis and prediction of protein domain functions. A.B. and T.M. performed mass spectrometry and data analysis. The manuscript was written by N.T. and R.S. All authors contributed to editing the manuscript and support the conclusions.

Competing interests

R.S. is a scientific co-founder and advisor of BiomX and Ecophage. All other authors declare no competing interests.

Additional information

Extended data is available for this paper at https://doi.org/10.1038/s41564-022-01158-0.

Supplementary information The online version contains supplementary material available at https://doi.org/10.1038/s41564-022-01158-0.

Correspondence and requests for materials should be addressed to Rotem Sorek.

Peer review information *Nature Microbiology* thanks Jayanta Chaudhuri and the other, anonymous, reviewer(s) for their contribution to the peer review of this work.

Extended Data Fig. 1 | See next page for caption.

Extended Data Fig. 1 | dCTP deaminases protect against phage infection. (A) Superposition of the C-terminal region (residues 351-550) of the AlphaFold-predicted structure of *E. coli* AW1.7 dCTP deaminase (turquoise), aligned with Streptococcus mutans cytosine deaminase (PDB: 2hvw) (grey). Zn^{2+} ions are depicted as blue spheres. Alignment was performed by PDBeFOLD61, with a Q score = 0.33, Z score = 9.0 and RMSD = 2.72 Å between the two structures. (B) Representative instances of cytidine deaminase genes (in turquoise) and their genomic neighborhoods. Genes known to be involved in defense are shown in yellow. RM, restriction modification; TAs, toxin-antitoxin systems; Septu and Hachiman are recently described defense systems14. The bacterial species and the accession of the relevant genomic scaffold in the Integrated Microbial Genomes (IMG) database47 are indicated on the left. (C) Bacteria expressing dCTP deaminases from *E. coli* U09 or *E. coli* AW1.7, as well as a negative control that contains an empty vector, were grown on agar plates in room temperature. Tenfold serial dilutions of the phage lysate were dropped on the plates. Data represent plaque-forming units per milliliter for ten phages tested in this study. Each bar graph represents average of three replicates, with individual data points overlaid. (D) Growth curves of cells expressing *E. coli* AW1.7 dCTP deaminase (turquoise), and control cells (grey). Results of three replicates are presented as individual curves.

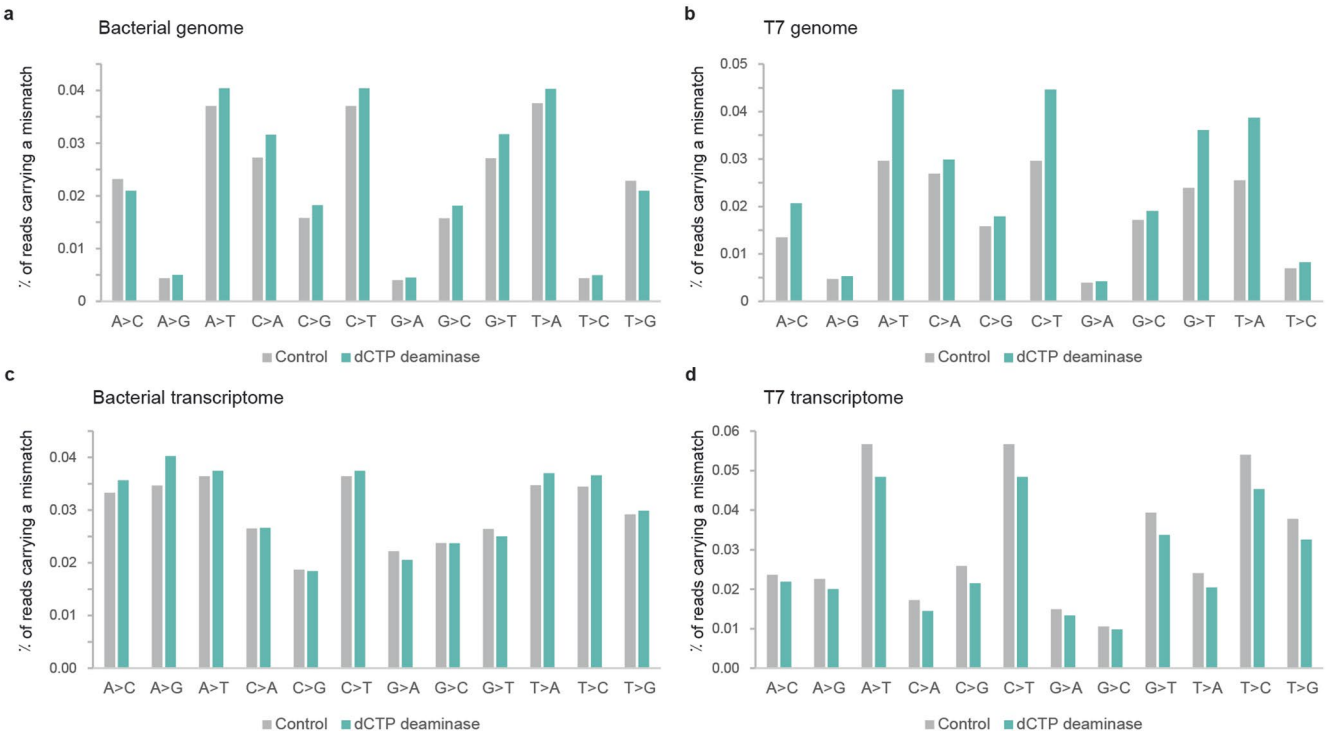

Extended Data Fig. 2 | No evidence for editing of genome and transcriptome by the dCTP deaminase. Cells expressing the deaminase from *E. coli* AW1.7 were infected by phage T7 at a multiplicity of infection (MOI) of 2 at 37 °C. Total DNA and total RNA were extracted after 15 minutes from the onset of infection, and were subjected to DNA-seq and RNA-seq, respectively. Panels A and B show the abundance of DNA reads with specific mismatches for reads aligned to the bacterial genome (A) or the phage genome (B). Panels C and D show the abundance of RNA-seq reads with specific mismatches for reads aligned to the bacterial genome (C) or the phage genome (D).

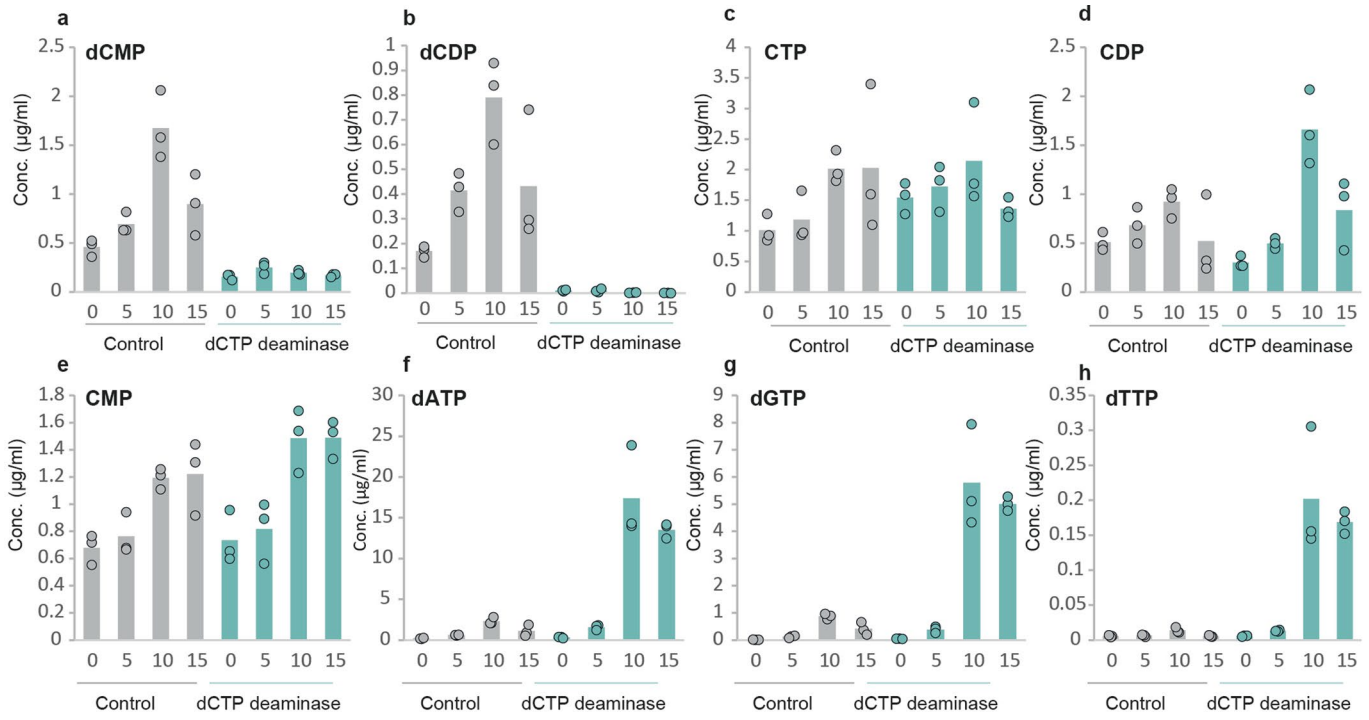

Extended Data Fig. 3 | Cellular nucleotides during phage infection. (A-H) Concentrations of various nucleotides in cell lysates extracted from T7-infected cells, as measured by LC-MS with synthesized standards. X axis represents minutes post infection, with zero representing non-infected cells. Cells were infected by phage T7 at an MOI of 2. Each panel shows data acquired for dCTP deaminase-expressing cells or for control cells that contain an empty vector. Bar graphs represent average of three biological replicates, with individual data points overlaid.

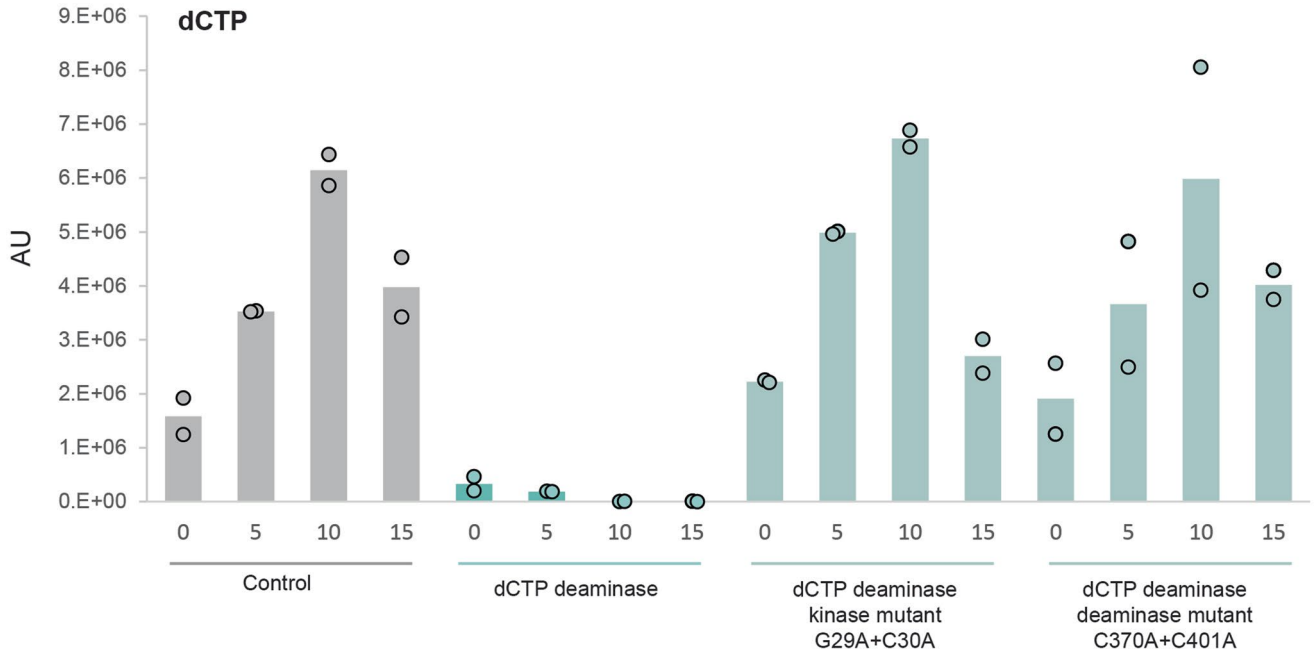

Extended Data Fig. 4 | Mutated dCTP deaminase does not elicit dCTP depletion. Relative abundance of dCTP in cell lysates extracted from T7-infected cells, as measured by LC-MS. X axis represents minutes post infection, with zero representing non-infected cells. Y axis represents the area under the peak for dCTP, in arbitrary units (AU). Cells were infected by T7 at an MOI of 2. Presented are data acquired for cells expressing the dCTP deaminase from *E. coli* AW1.7, control cells that contain an empty vector, or cell expressing mutated forms of the dCTP deaminase. Bar graphs represent average of two biological replicates, with individual data points overlaid.

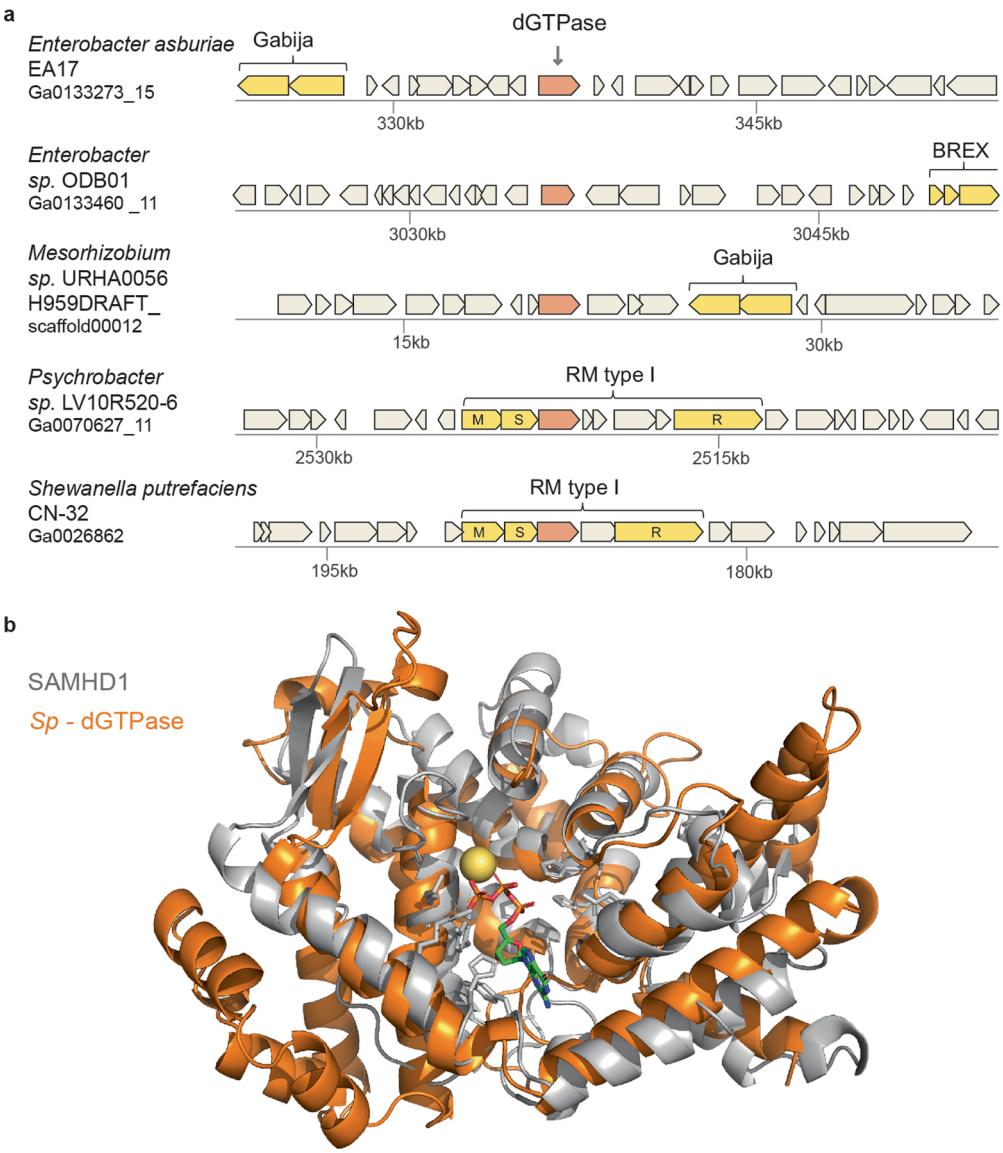

Extended Data Fig. 5 | A family of dGTPases in defense islands. (A) Representative instances of dGTPase genes (in orange) and their genomic neighborhoods. Colors and annotations are as in Supplementary Fig. S1A. M, S and R designations within type I RM operon genes represent the methylase, specificity, and restriction subunits, respectively. (B) Superposition of the AlphaFold predicted structural model of Sp-dGTPase (orange) aligned with the N-terminus of the human SAMHD1 (PDB: 4bzb, chain D) (grey). Mg^{2+} ion is depicted as a yellow sphere. SAMHD1 catalytic site is depicted with grey sticks, and is bound to the dGTP ligand. Alignment was performed by PDBeFOLD, with a Q score = 0.11, Z score = 5.5 and RMSD = 2.89 Å between the predicted dGTPase AlfaFold2 model and the human SAMHD1. The presented structural alignment includes residues 23–161 & 248–452 from the dGTPase AlphaFold model, aligned to residues 129–275 & 299–439 of the human SAMHD1 structure.

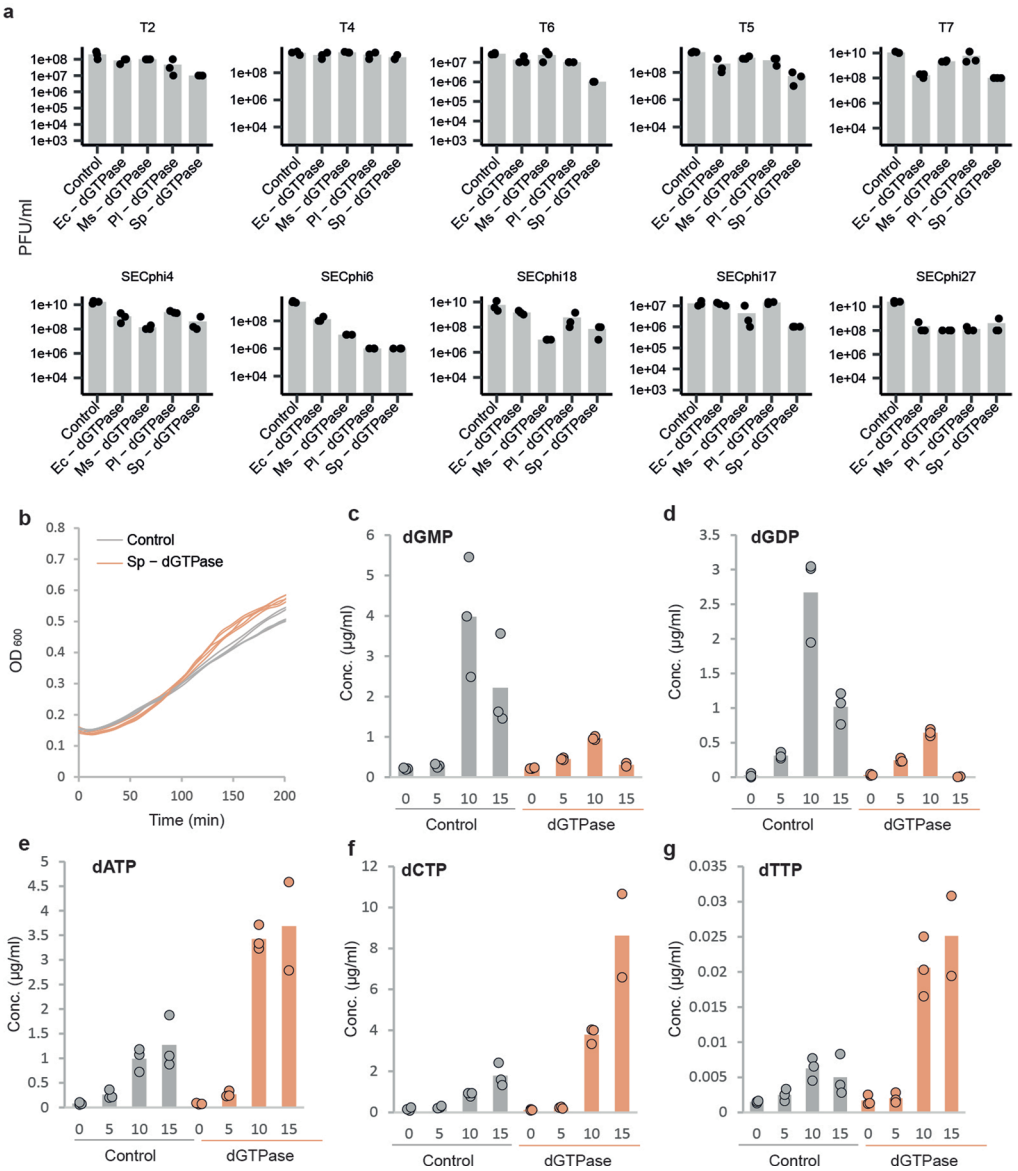

Extended Data Fig. 6 | dGTPases protect against phage infection. (A) E. coli MG1655 cells expressing dGTPases cloned under an arabinose-inducible promoter from several species (Ec, *E. coli* G177; Ms, Mesorhizobium sp. URHA0056; Pl, Pseudoalteromonas luteoviolacea DSM6061; Sp, Shewanella putrefaciens CN-32), as well as a negative control, were grown on agar plates in room temperature in the presence of 0.2% arabinose. Tenfold serial dilutions of the phage lysate were dropped on the plates. Data represent plaque-forming units per milliliter for phages tested in this study. Each bar graph represents average of three replicates, with individual data points overlaid. (B) Growth curves of cells over-expressing the Sp-dGTPase gene from Shewanella putrefaciens CN-32 (orange) and control cells (grey) following 0.2% arabinose induction. Results of four replicates are presented as individual curves. Expression of the Sp-dGTPase protein was verified via protein mass spectrometry. (C-G) Concentrations of deoxynucleotides in cell lysates extracted from T7-infected cells, as measured by LC-MS with synthesized standards. X axis represents minutes post infection, with zero representing non-infected cells. Cells were infected by phage T7 at an MOI of 2. Each panel shows data acquired for dGTPase-expressing cells or for control cells that express GFP. Bar graphs represent average of three biological replicates (or two replicates for the dGTPase samples at t = 15 mins), with individual data points overlaid.

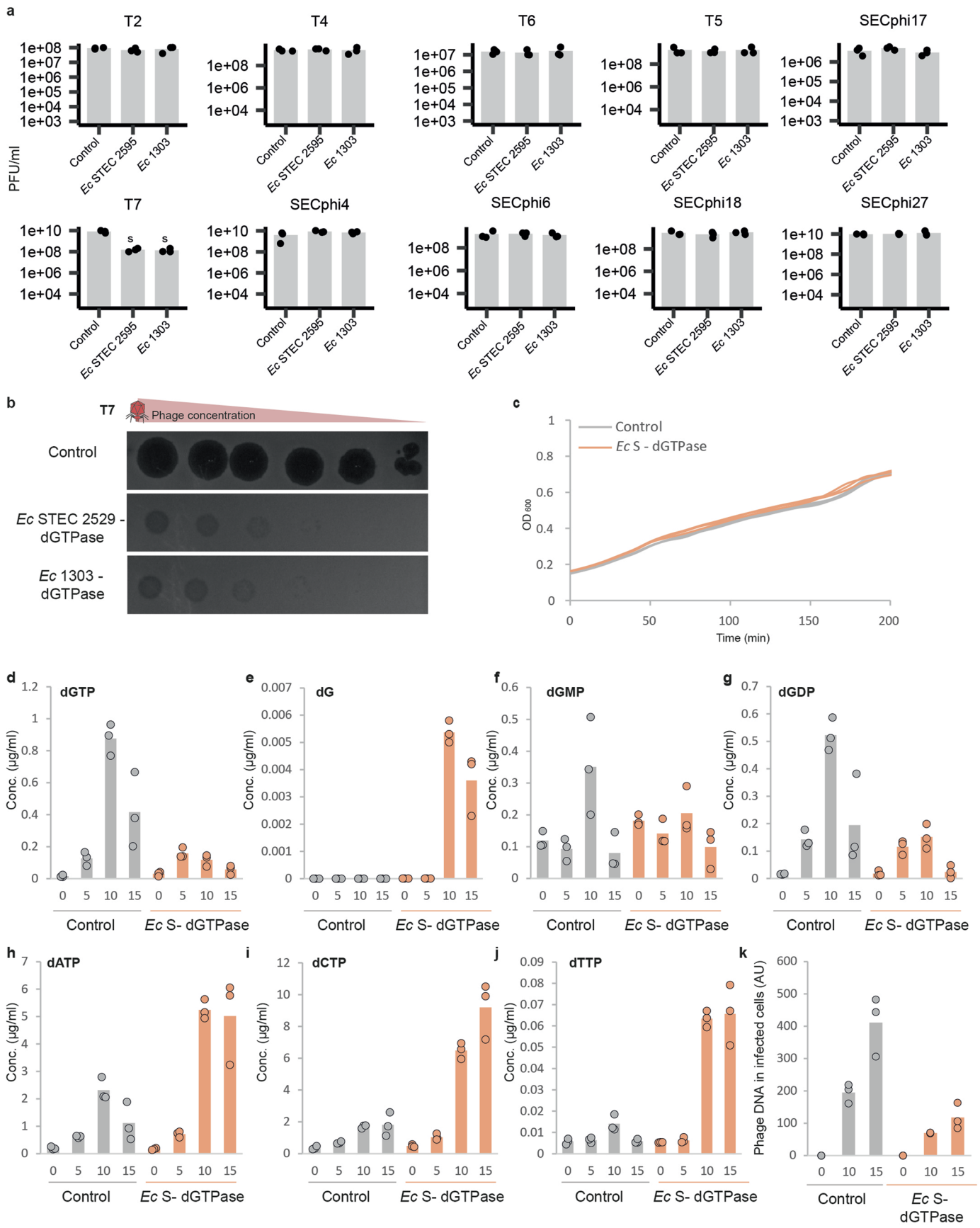

Extended Data Fig. 7 | See next page for caption.

Extended Data Fig. 7 | dGTPases cloned under native promoters protect against phage infection. (A) E. coli MG1655 cells containing dGTPases cloned, together with their native promoters, from two different *E. coli* strains (Ec S, *E. coli* STEC 2595; Ec 1303, *E. coli* 1303), as well as a negative control, were grown on agar plates in room temperature. Tenfold serial dilutions of the phage lysate were dropped on the plates. Data represent plaque-forming units per milliliter for tested phages. Each bar graph represents average of three replicates, with individual data points overlaid. (B) T7 defense by dGTPases expressed from native promoters. Shown are ten-fold serial dilution plaque assays, comparing the plating efficiency of T7 phage on bacteria that express the Ec STEC 2529, Ec 1303 or a control strain that lacks the gene. Images are representative of three replicates. (C) Growth curves of cells harboring the Ec S - dGTPase gene from *E. coli* STEC 2595 (orange) and control cells with an empty plasmid (grey). Results of three replicates are presented as individual curves. (D-J) Concentrations of deoxynucleotides in cell lysates extracted from T7-infected cells, as measured by LC-MS with synthesized standards. X axis represents minutes post infection, with zero representing non-infected cells. Cells were infected by phage T7 at an MOI of 2. Each panel shows data acquired for cells expressing the Ec S dGTPase or for control cells containing an empty pSG1 vector. Bar graphs represent average of three biological replicates, with individual data points overlaid. (K) Effect of native dGTPase expression on T7 DNA replication throughout infection. Cells were infected by phage T7 at an MOI of 2 at 37 °C. Total DNA was extracted from each sample and DNA was Illumina-sequenced. Each panel shows data acquired for Ec-S-expressing cells or for control cells that contain an empty vector. Y axis represents phage DNA sequence reads normalized to reads from spiked-in DNA. Bar graphs represent the average of three biological replicates, with individual data points overlaid.

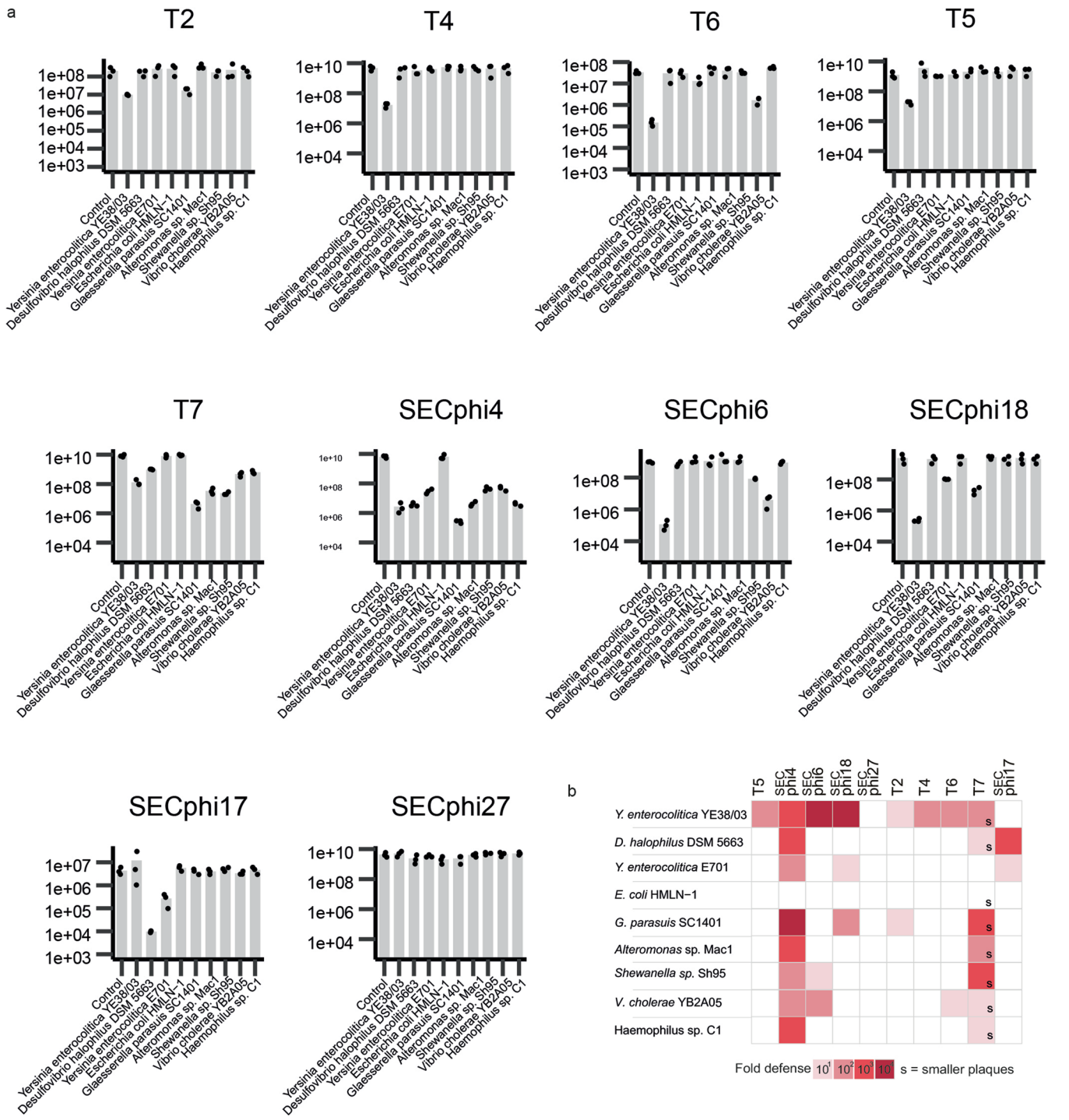

Extended Data Fig. 8 | Distant homologs of Sp-dGTPase protect against phage infection. (A) Bacteria expressing dGTPase cloned from multiple species (Yersinia enterocolitica YE38/03, Desulfovibrio halophilus DSM 5663, Yersinia enterocolitica E701, *Escherichia coli* HMLN-1, Glaesserella parasuis SC1401, Alteromonas sp. Mac1, Shewanella sp. Sh95, Vibrio cholerae YB2A05, Haemophilus sp. C1), as well as a negative control, were grown on agar plates in room temperature in the presence of 0.2% arabinose. Tenfold serial dilutions of the phage lysate were dropped on the plates. Data represent plaque-forming units per milliliter for tested phages. Each bar graph represents average of three replicates, with individual data points overlaid. (B) A summary of the defense results from the presented bar graphs.

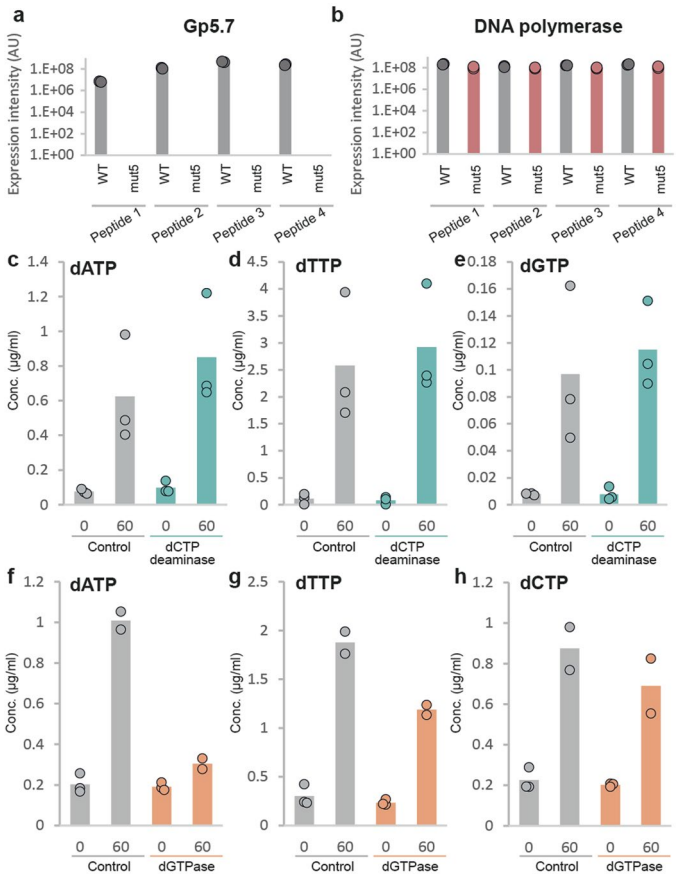

Extended Data Fig. 9 | Mutation verification of Gp5.7 and rifampicin treatment. (A) Verification of the absence of Gp5.7 in T7 mutant n. 5 using mass spectrometry. Peptide fragments of Gp5.7 identified by protein mass spectrometry of cells 15 minutes post infection by WT T7 and T7 mutant n.5 (MOI = 2). Multiple peptides of Gp5.7 are observed in the WT T7, but no peptides are detected in the mutant T7, supporting that the mutant does not express Gp5.7. Peptide fragments are as follows: peptide 1: GHISCLTTSGR, peptide 2: NGGAWEITASGTR, peptide 3: NNASLVAEAASR, peptide 4: TFQSNYVR. Bar graphs represent average of two biological replicates, with individual data points overlaid. (B) As control to the measurements in panel A, shown are peptide fragments of the T7 RNA polymerase identified by protein mass spectrometry in cells 15 minutes post infection. The T7 RNA polymerase is readily identified in both WT and mutant phages. Peptide 1: EQLALEHESYEMGEAR, peptide 2: MNTINIAK, peptide 3: SVMTLAYGSK, peptide 4: VLAVANVITK. Bar graphs represent average of two biological replicates, with individual data points overlaid. (C-H) Concentrations of dNTP nucleotides in cell lysates extracted from rifampicin-treated cells, as measured by LC-MS with synthesized standards. X axis represents minutes post treatment, with zero representing non-treated cells. (C-E) Each panel shows data acquired for dCTP deaminase-expressing cells or for control cells that contain an empty vector. Bar graphs represent average of three biological replicates, with individual data points overlaid. (F-H) Each panel shows data acquired for dGTPase-expressing cells or for control cells that express GFP. Bar graphs represent average of three biological replicates, with individual data points overlaid. In panels D-F, 60 minute data represent the average of two biological replicates.

nature portfolio

Corresponding author(s): rotem.sorek@weizmann.ac.il

Last updated by author(s): April 4, 2022

Reporting Summary

Nature Portfolio wishes to improve the reproducibility of the work that we publish. This form provides structure for consistency and transparency in reporting. For further information on Nature Portfolio policies, see our Editorial Policies and the Editorial Policy Checklist.

Statistics

For all statistical analyses, confirm that the following items are present in the figure legend, table legend, main text, or Methods section.

n/a	Confirmed
☐	☒ The exact sample size (*n*) for each experimental group/condition, given as a discrete number and unit of measurement
☐	☒ A statement on whether measurements were taken from distinct samples or whether the same sample was measured repeatedly
☒	☐ The statistical test(s) used AND whether they are one- or two-sided *Only common tests should be described solely by name; describe more complex techniques in the Methods section.*
☒	☐ A description of all covariates tested
☒	☐ A description of any assumptions or corrections, such as tests of normality and adjustment for multiple comparisons
☐	☒ A full description of the statistical parameters including central tendency (e.g. means) or other basic estimates (e.g. regression coefficient) AND variation (e.g. standard deviation) or associated estimates of uncertainty (e.g. confidence intervals)
☒	☐ For null hypothesis testing, the test statistic (e.g. *F*, *t*, *r*) with confidence intervals, effect sizes, degrees of freedom and *P* value noted *Give P values as exact values whenever suitable.*
☒	☐ For Bayesian analysis, information on the choice of priors and Markov chain Monte Carlo settings
☒	☐ For hierarchical and complex designs, identification of the appropriate level for tests and full reporting of outcomes
☒	☐ Estimates of effect sizes (e.g. Cohen's *d*, Pearson's *r*), indicating how they were calculated

Our web collection on statistics for biologists contains articles on many of the points above.

Software and code

Policy information about availability of computer code

Data collection	Plate reader data was collected using a Tecan Infinite 200 instrument with Tecan iControl v3.8.2.0 software.
Data analysis	NovoAlign (Novocraft) v3.02.02 Breseq (versions 0.29.0 or 0.34.1) Clustal-Omega (version 1.2.4) hhsearch' option of hhsuite (version 3.0.3) MMseqs2 (release 12-113e3, release 2-1c7a89, release 6-f5a1c) FastTree (2009) iTOL v4

For manuscripts utilizing custom algorithms or software that are central to the research but not yet described in published literature, software must be made available to editors and reviewers. We strongly encourage code deposition in a community repository (e.g. GitHub). See the Nature Portfolio guidelines for submitting code & software for further information.

Data

Policy information about availability of data

All manuscripts must include a data availability statement. This statement should provide the following information, where applicable:

- Accession codes, unique identifiers, or web links for publicly available datasets
- A description of any restrictions on data availability
- For clinical datasets or third party data, please ensure that the statement adheres to our policy

Genomes analyzed in this study were downloaded from Integrated Microbial Genomes (IMG) database, October 2017. Gene sequences were retrieved from the

IMG data base. All accession numbers are available in the Methods section and Supplementary Tables.
The datasets generated during and/or analyzed during the current study are available from the corresponding author on reasonable request.

Field-specific reporting

Please select the one below that is the best fit for your research. If you are not sure, read the appropriate sections before making your selection.

☒ Life sciences ☐ Behavioural & social sciences ☐ Ecological, evolutionary & environmental sciences

For a reference copy of the document with all sections, see nature.com/documents/nr-reporting-summary-flat.pdf

Life sciences study design

All studies must disclose on these points even when the disclosure is negative.

Sample size	Experiments were performed in triplicates without prior sample size calculation, as is standard for such experimental designs.
Data exclusions	In Figure 2 D-E, two replicates are presented for the 15 minutes time point. A third replicate couldn't be collected as one flask broke during this experiment.
Replication	Experiments were performed in triplicates as is standard for such experimental designs. No failed replications occurred.
Randomization	Randomization was used for sample injection order in mass spectrometry measurements. Randomization is not standard for the other experiments performed.
Blinding	Blinding is not standard for the experiments performed

Reporting for specific materials, systems and methods

We require information from authors about some types of materials, experimental systems and methods used in many studies. Here, indicate whether each material, system or method listed is relevant to your study. If you are not sure if a list item applies to your research, read the appropriate section before selecting a response.

Materials & experimental systems

n/a	Involved in the study
☒	☐ Antibodies
☒	☐ Eukaryotic cell lines
☒	☐ Palaeontology and archaeology
☒	☐ Animals and other organisms
☒	☐ Human research participants
☒	☐ Clinical data
☒	☐ Dual use research of concern

Methods

n/a	Involved in the study
☒	☐ ChIP-seq
☒	☐ Flow cytometry
☒	☐ MRI-based neuroimaging